University of Nevada

Reno

Structural-Tectonic Analysis of Northern Dixie Valley, Nevada

A thesis submitted in partial fulfillment of the requirement for the degree of Master of Science in Geology

by

Robert A. Whitney

July 1980

ABSTRACT

Structural-tectonic and surficial geologic studies of northern Dixie Valley, Nevada, using photogeologic methods, indicate the valley is a complex asymmetric graben bounded by high-angle Basin and Range faults. The graben asymmetry is the expression of a main fault system bounding the northwest side of the valley and several step faults bounding the southeast side. The surficial geology on the valley floor expresses the asymmetric graben model. Re-activation of pre-Basin and Range faults and Basin and Range faulting may be in response to late Cenozoic regional extension below the Moho. The extension may result in decoupling of the upper crust by listric normal faulting, tilting of mountain blocks, and graben formation.

CONTENTS

CONTENTS (Cont.)

FIGURES

FIGURES (Cont.)

PLATES
(in pocket)

INTRODUCTION

Purpose and Scope

Northern Dixie Valley, Nevada, has been designated a "known geothermal resource area" from geothermal discoveries in preliminary development of the area by Sun Oil Company. This study was undertaken to develop a structural-tectonic framework for northern Dixie Valley to aid in developing the geothermal resource by defining a model for the geothermal system. The area of geothermal interest is shown on Figure 1 and Plate I.

The study was conducted in two stages: Stage I included evaluation of available geologic and geophysical data including published data and existing imagery from various sources; Landsat, SKYLAB, NASA underflights, AMS photography, and existing low-sun angle (LSA) photography.

Stage II consisted of conducting a LSA photographic program of the study area, interpreting the resultant photography and field checking the photogeologic data. Field work also included a preliminary fault scarp morphology study and a compilation of a generalized surficial geologic map of the study area.

Methods and Analytical Techniques

Literature search

The literature search was conducted primarily at the library of the University of Nevada-Reno, but included

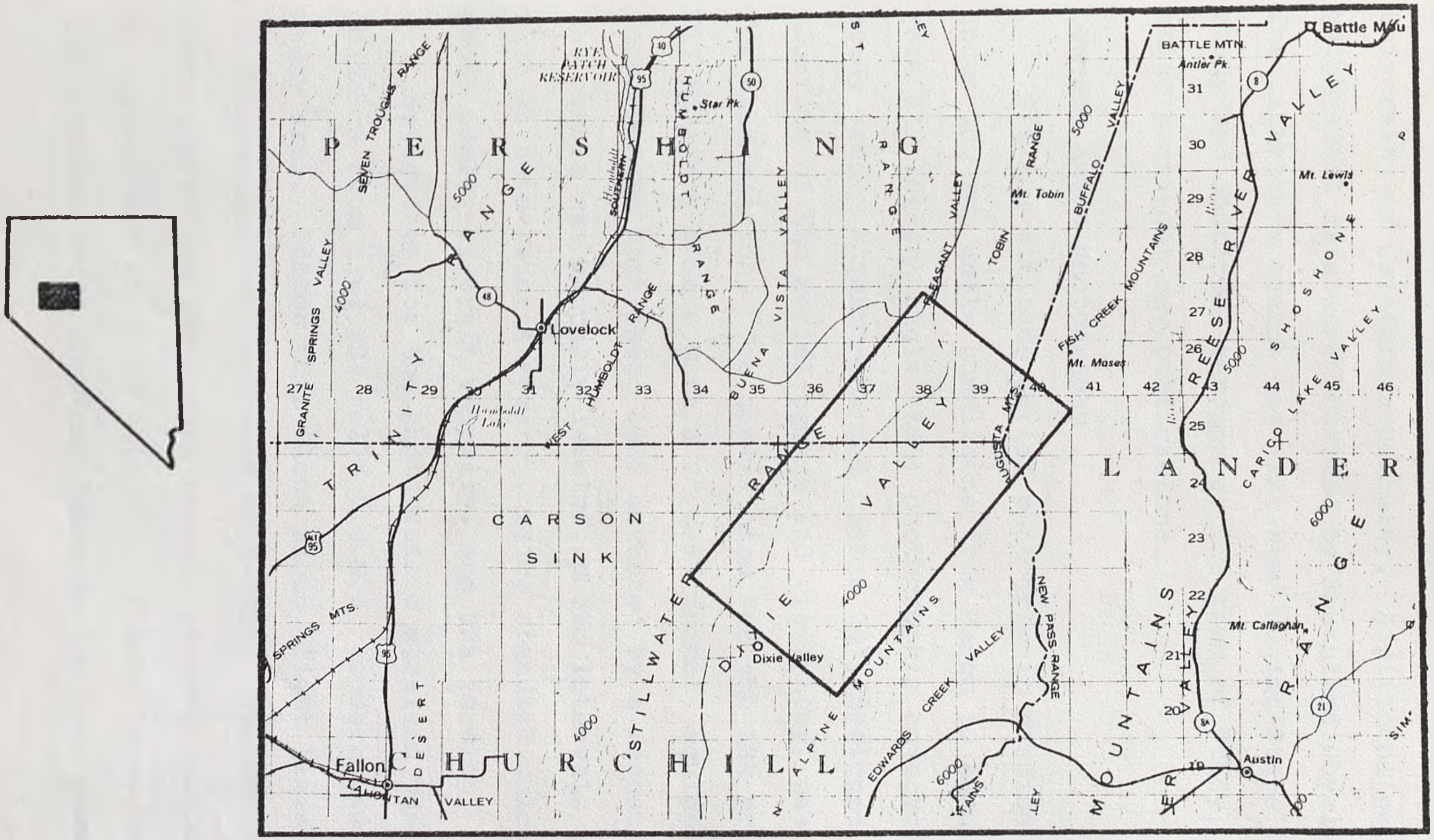

Figure 1. Location map of the study area.

additions to the reference bibliography from a limited computer search conducted by the Lawrence Livermore Laboratory, University of California-Berkeley. Additional geologic and geophysical data were provided by Southland Royalty Company. The literature search was initiated during Stage I of the study and continued throughout the term of study, incorporating pertinent new publications.

Low-sun angle photography

Six low altitude aerial photographic missions were flown under low-sun angle conditions from March to August, 1979, to generate low-sun angle (LSA) photographic coverage of the study area. A turbo-charged Cessna 207, designed for in-cabin mounting of the aerial camera and viewfinder, was chartered for each mission. The camera used for the LSA program was a K17 military camera with a 9" x 9" format, equipped with a 6" focal length high speed lens actuated by a mechanical switch. The camera was manually leveled, photo intervals were timed with an auto-reset stopwatch, using standard calculations for photo scale, aircraft velocity, and 60% forelap.

Navigation for the photographic missions was by inflight guidance from 1:62,500 scale U.S.G.S. topographic maps of the study area. Photos were flown along flight lines subparallel to the regional structure of N31E-S31W. Flight altitude of about 6,000 feet above mean terrain yielded photography with an approximate scale of 1:12,000. Flight lines were spaced 1 5/16 miles apart to yield 20% side lap with photo intervals timed to yield 60% forelap to provide adequate stereoscopic images.

Kodak Tri-X (#2403) high speed black and white aerographic film was used for the first four missions and Kodak Double-X (#2405) black and white aerographic film was used for the last two missions. The film was commercially processed and printed by American Aerial Survey, Inc., of Sacramento, California. A total of 1324 LSA images of good to excellent quality were obtained for the study area. An index of these images is incorporated into Plate II.

Flight times to obtain optimal results from LSA photography are defined by Slemmons (1969) and Glass and Slemmons (1978) as the two-hour interval beginning one-half hour after sunrise and the two-hour interval ending one-half hour before sunset. These optimum time intervals were used for the LSA program in Dixie Valley.

Seasonal variations in sun azimuth indicated an early spring program for optimum LSA imagery with respect to the regional trends in Dixie Valley (Slemmons, 1969; Glass and Slemmons, 1978; Slemmons, personal communication, 1979). Approximately 90% of the imagery was obtained in early March under optimal conditions, with follow-up flights conducted in June and August.

Slemmons (1969) and Glass and Slemmons (1978) summarize the advantage of using highlighting techniques versus shadowing techniques for structural enhancement. The latter was used where possible in the program to detect very subtle structural features.

Interpretation of all stereoscopic images (LSA, NASA, and AMS imagery) was accomplished with a Wild ST-4 stereoscope. Structural and tectonic photographic interpretations were delineated on mylar overlays on alternate images and then transferred to preliminary 7 1/2 minute topographic quadrangle sheets (1:24,000 scale) with the aid of a Bausch and Lomb Zoom Stereo Scope. These map sheets were reduced by Photo-Mechanical Transfer (PMT) and assembled into a composite map (Plate II). Field verification of structural interpretations were conducted during the summer and fall of 1979, and the spring of 1980.

Snow-lapse photography

Snow-lapse photography planned for the winter months of late 1978 and 1979 in an effort to delineate areas of high heat flow by determining snow melt rates, was not accomplished. Major regional snowstorms occurred on December 19 and 20, 1978, and on February 22 and 23, 1979. Aerial reconnaissance flights immediately following the two storms (December 20, 1978, and February 23, 1979) verified the lack of adequate snow cover in Dixie Valley to accomplish a snow-lapse study.

A Landsat imagery search for images dated immediately following regional storms also verified the lack of snow cover in Dixie Valley following major storms. An image dated December 20, 1978 (Figure 2), shows the results of a regional storm which included 90% or greater snow cover in west

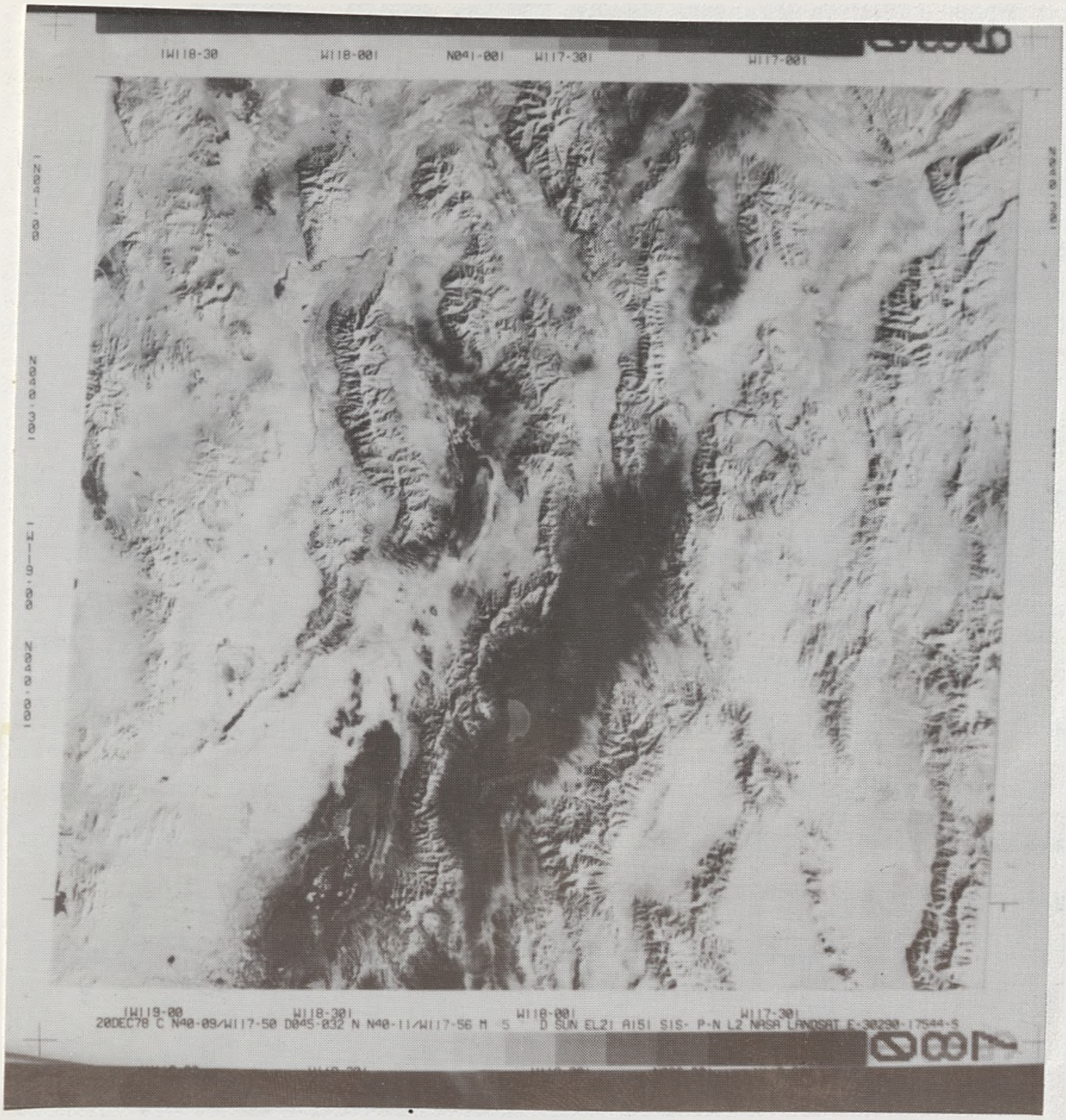

Figure 2. Landsat image of December 20, 1979 of north-central Nevada following a regional snowstorm. Area in center without snow cover is Dixie Valley.

central Nevada. Dixie Valley is in the 10% without snow cover. This situation, which seems to recur after most regional storms, may be the result of local climatic influences (Dixie Valley has a low elevation for the Great Basin area) or may represent a valley wide area of high heat flow reflecting the underlying geothermal system.

Surficial geology

Generalized surficial geology of northern Dixie Valley was delineated by interpretation of black and white 1:62,500 scale AMS photographs, with refinements based upon the 1:12,000 scale LSA photography. Because the various surficial geologic units correspond with specific geomorphic surfaces that also indicate genetic origin of the units, the surficial geology is presented as a generalized geomorphic surfaces map (Plate III). Surface and near-surface samples of the various units were collected for grain-size analysis and the results are presented in Appendix A.

Fault scarp morphology studies

Fault scarp morphology studies were conducted within the study area on scarps delineated from interpretation of the LSA photography. The methods of Wallace (1977 and unpublished data) and Bucknam and Anderson (1979) were used. Only fault scarps in excess of 1 m height and with moderate to steep slopes were chosen for profiling. The scarps were profiled by laying a stadia rod directly on the scarps and measuring the length and inclination of each portion of the fault. Terminology of fault scarp morphology developed by Wallace (1977) is shown in Figure 3. Results of this study are incorporated into the structural-tectonic analysis. Location of the scarp profiles are shown on Plate IV and the profiles are in Appendix B.

Geophysical analysis

A geophysical analysis of the study area was accomplished using published gravity and aeromagnetic studies in northern Dixie Valley and unpublished aeromagnetic studies supplied by Southland Royalty Company. A reinterpretation of this data is incorporated into the structural-tectonic analysis.

Previous Work

Numerous researchers have conducted studies within the Dixie Valley region. Only those papers in the various critical disciplines that have contributed most to the present study are mentioned here. Active faulting in the Dixie Valley and nearby areas was studied by Larson (1957), Slemmons (1957), Slemmons and others (1957), Burke (1967), Ryall and Malone (1971), and Wallace (1978, 1980a, 1980b). Regional studies were conducted by Stewart (1971, 1977, 1978), Thompson and Burke (1974), Wright (1976), Speed (1976), Hamilton (1978), Dickinson (1977, 1979), Eaton and others (1978), and Eaton (1979).

Geologic maps of the Dixie Valley area were prepared by

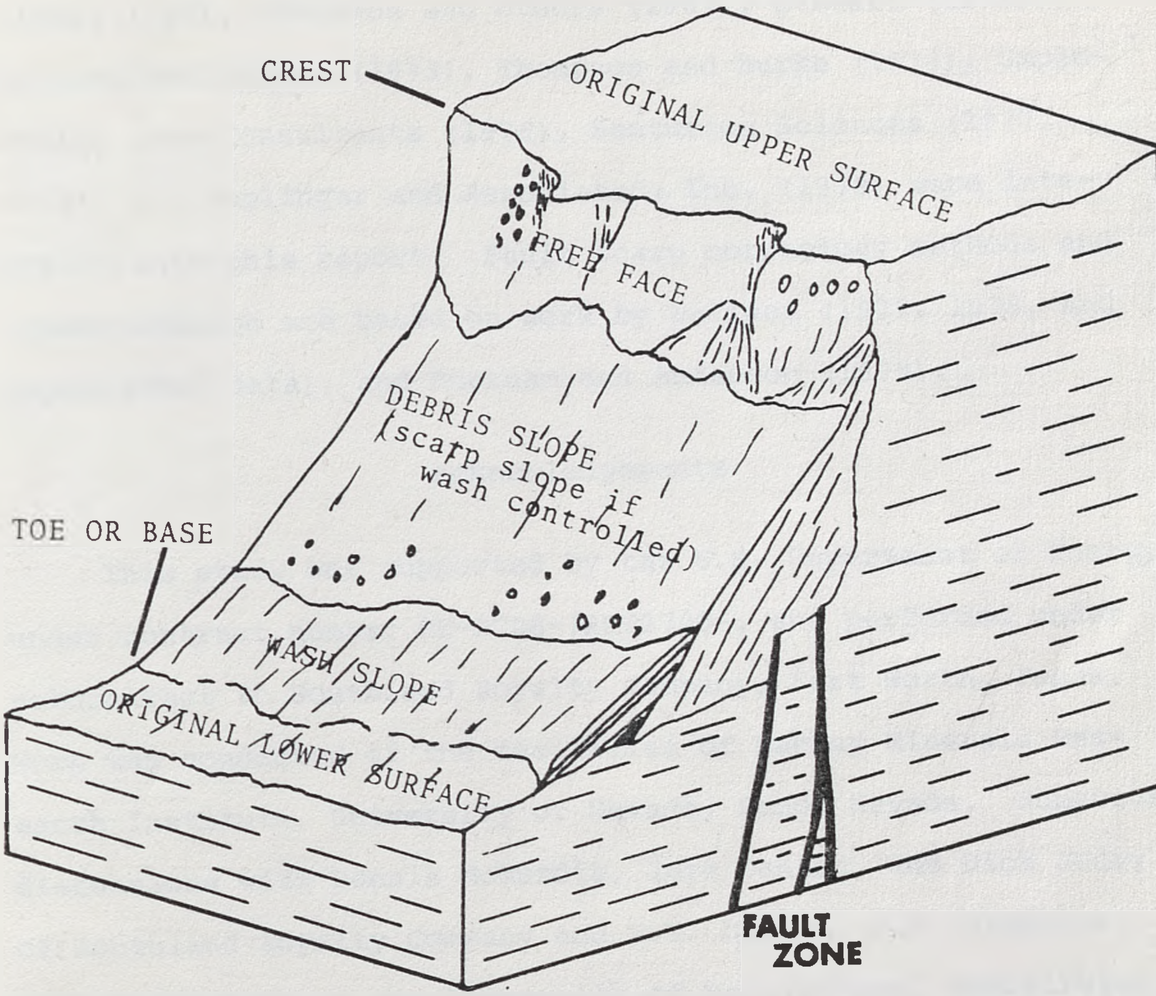

Figure 3. Block diagram of a fault scarp showing terminology used in fault scarp morphology studies (Wallace, 1977).

Page (1965), Willden and Speed (1974), and Johnson (1977). Geophysical and seismological data of Meister (1967), Smith (1967, 1968), Thompson and others (1967), Stewart (1971), Koizumi and others (1973), Thompson and Burke (1974), Exploration Data Consultants (1976), Senturion Sciences (1977, 1978), and Keplinger and Associated, Inc. (1978) were integrated into this report. Fault scarp morphology methods and interpretation are based on work by Wallace (1977, 1978, and unpublished data), and Bucknam and Anderson (1978).

Acknowledgements

This study was supported by the U.S. Department of Energy under contract number DE-AC08-79ET27006, and performed under subcontract to Southland Royalty Company, Fort Worth, Texas. Work was conducted at the facilities of Mackay Minerals Research Institute, University of Nevada, Reno, Nevada. Numerous discussions with Dennis McMurdie, Jere Denton, and Dick Jodry of Southland Royalty Company and L.T. Larson, D.B. Slemmons, and Elaine Bell of the University of Nevada-Reno, contributed to the development of the ideas and helped to focus the investigations of the structural-tectonic and geologic character of Dixie Valley as expressed in this thesis. Capable field assistance was provided by Tom Bard, Russell Juncal, Anne Zelinski, Anna Evasko Jamison, Cady Johnson, Neil Ingraham, and Rod Fricke of the University of Nevada-Reno. Grain-size analyses of selected surficial deposit samples conducted by Anne Zelinski are gratefully incorporated into this report.

Appreciation is extended to the many photogeology students at UNR who assisted on the photographic missions; and to Frank Elliott and Pat Miller, pilots for Aviation Services, Inc., for always putting the plane on course and making it home on "empty". Technical and editorial review by University of Nevada-Reno and Southland Royalty Company personnel, in particular, Dennis McMurdie, Burt Slemmons, Larry Larson, and Elaine Bell, significantly improved this thesis. Final typing by Loni Harriet was essential for report completion.

REGIONAL GEOLOGIC SETTING AND TECTONIC HISTORY

Regional Setting

Northern Dixie Valley is within the west-central portion of the Basin and Range structural and geomorphic province (Figure 4). The region is characterized by north-northeast trending mountain ranges (horsts) and intervening valleys (grabens). The mountain ranges are bounded by high angle normal faults, which have generally tilted the mountain ranges gently to the southeast (Stewart, 1971; Wallace, 1980a). The valleys contain alluvial fill derived from adjacent bedrock areas to depths of several thousand feet.

Precambrian and Paleozoic Tectonic History

Rifting of a tectonic block between 750 and 850 million years ago (mya) removed all older deposits from the west margin of the North American plate and triggered an episode of miogeosynclinal deposition (Dickinson, 1977) along the newly formed western margin, about the eastern edge of the present Basin and Range Province. This miogeosynclinal regime continued through the Paleozoic with only minor interruptions in the late Paleozoic. Thick sequences of highly metamorphosed Precambrian and Cambrian shelf lie along the rifted margin and include: (1) diamictite, mudstone, sandstone, conglomerate and mafic volcanics of Precambrian age, (2) Upper Precambrian and lower Cambrian detrital rocks of shallow marine (including tidal) origin and (3) a middle

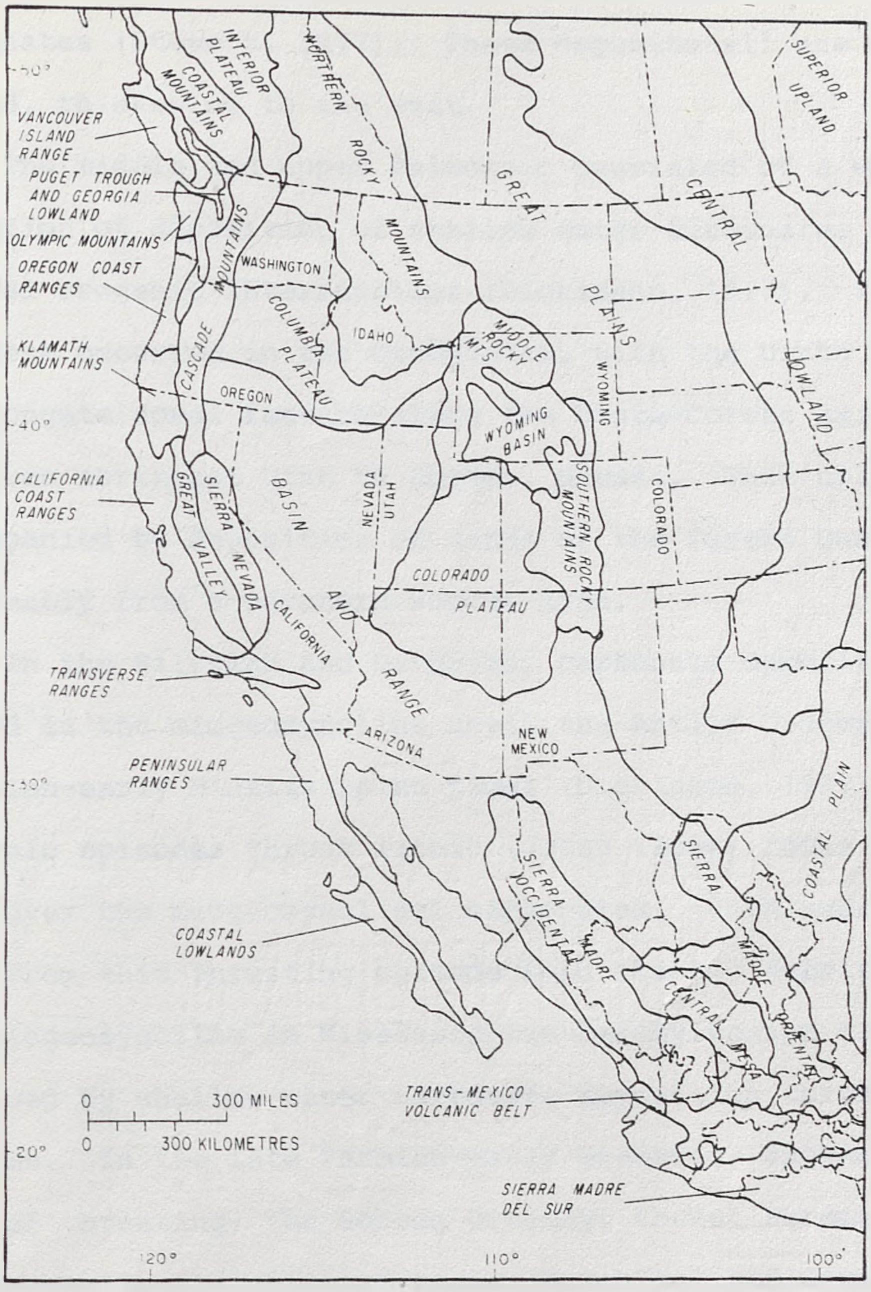

Figure 4. Geomorphic provinces map of the western United States (Stewart, 1978).

and upper Cambrian sequence of predominately shallow water carbonates (Stewart, 1977). These deposits all are wedged shaped, thickening to the west.

The middle and upper Paleozoic consisted of a westward migration of deposition of shallow water carbonates with several orogenic interruptions (Dickinson, 1977). The first of these occurred in the Ordovician, with the Uinta Uplift, an elongate domal feature along the Uinta-Cortez axis reaching from northeast Utah to Cortez, Nevada. This uplift was accompanied by deposition of sands of the Eureka Quartzite, presumably from a northern source area.

In the Silurian and Devonian, carbonate deposition persisted in the miogeosyncline until the Antler Orogeny of late Devonian-early Mississippian times (Dickinson, 1977). These orogenic episodes thrust lithic (ocean floor) rocks to the east over the miogeosynclinal carbonates. Highlands resulting from this thrusting episode shed clastic debris into the miogeosyncline in Mississippian-Pennsylvanian times, followed by shallow water carbonate deposition through the Permian. In the late Permian-early Mesozoic, another episode of thrusting, the Sonoma Orogeny, thrust Permian and earlier sediments eastward again (Burchfiel and Davis, 1975; Dickinson, 1977).

The eastward thrusting of deeper oceanic facies rocks, such as the Slaven Chert and the Vinini and Valmy Formations effectively removed Paleozoic sediments from the study area, thrusting them eastward onto the shelf.

Opening and closing of a marginal sea behind an island arc is considered to be the driving mechanism for these thrusting episodes (Packham and Falvey, 1971). In their model, island arc systems are continually rifted from and re-collided with continental margins by asymmetric rifting within the marginal sea and migration of the subduction zone from under the island arc to under the edge of the continent. These episodes effectively destroy at least the deeper part of the marginal sea by subduction, thrusting the accumulated deeper sediments over the shelf and slope deposits on the continental shelf. The collision is followed by re-rifting of the island arc for the edge of the craton, recreating a marginal sea environment.

Mesozoic Tectonic History

In the west-central Basin and Range Province, marginal sea and associated island arc deposition persisted until mid to late Triassic times. At this time, the island arc was accreted to the continent (Dickinson, 1977).

Triassic and Jurassic subduction migrated westward in several steps, represented by the Sierra Nevada Mountains and the Coast Ranges in California. Deep marginal sea deposition continued in the west-central Basin and Range, accompanied by intrusive episodes and volcanics. Regional uplift of the Basin and Range began in the Jurassic and the region became subaerial by the Cretaceous (Hamilton, 1978). The late Cretaceous Laramide Orogeny deformed rocks further east, closer to the craton than the study area in west-central Nevada. Cretaceous granitic intrusions are widespread in the western Basin and Range.

The mechanism for the emplacement of widespread Cretaceous intrusions in the Basin and Range was an eastward advance of the deeper portion of the subduction zone from the area of the Sierra Nevada to under the Rocky Mountains. Effectively, this moved the point in the subduction zone at which partial melting of the subducted slab occurred to the east. An increase in the collision rate between the North American and Farallon plates of from 10 cm to 14 cm per year, which decreases the angle of the subduction zone, is suggested as a reason for this migration (Dickinson, 1979).

Cenozoic Tectonic History

The Laramide Orogeny continued into the Paleogene. About 40 mya the collision of the North American and Farallon plates slowed and the angle of the subduction zone increased, effectively migrating the depth of partial melting westward again. This ended the Laramide Orogeny and caused extensive intrusive emplacement and acidic volcanism between the Rocky Mountains and the Sierra Nevada between 40 and 20 mya (Dickinson, 1976, 1979).

Subduction continued into the Neogene along the west coast building an Andean type arc. About 22 mya, the Farallon-East Pacific ridge began to be consumed by angular collision, with the subduction system. Upon consumption of the ridge system, the west coast became a transform margin--the San Andreas fault-bounded by triple junctions. As more of the ridge was consumed by the angular collision, the triple points moved north and south, lengthening the San Andreas transform (Atwater, 1970; Dickinson, 1977).

Mid-Miocene (15-17 mya) marks the inception of extensional Basin and Range faulting (Stewart, 1971). The Sierra Nevadan Orogeny which began in late Jurassic had by this time reached a high enough elevation to close the Great Basin to oceanic drainage.

Extensional faulting began in the southern portions of the Basin and Range, southern California, Arizona, New Mexico, and was approximately inland from the bounding triple points of the early San Andreas system.

As more of the ridge was consumed, the bounding triple points of the San Andreas moved north and south, increasing the transform margin length to that of the present. As the length increased, the area inland subject to extensional faulting enlarged (Dickinson, 1979). Inception of the Garlock fault, a left-lateral continental transform apparently relieved the effects of extensional tectonics in the southern Basin and Range. Extension was accompanied by a late Tertiary-early Quaternary episode of basaltic and bimodal basaltic-rhyolitic volcanism throughout most of the northern Basin and Range (Stewart, 1978; Dickinson, 1979).

Present Structural-Tectonic Regime

The structural-tectonic setting in the Basin and Range is the result of brittle fracture in a thin crust in response to extension at depth. Extension may be caused by the northwestward movement of the Sierra Nevada block relative to the stable Colorado Plateau and Rocky Mountain Provinces (Atwater, 1970; Wright, 1976; Stewart, 1978; Eaton and others, 1978). This extension has occurred at sporadic rates for the last 15 to 17 million years and has resulted in a widening of the province by about 160 km (Stewart, 1971). Eaton and others (1978) report from 10% to 30% roughly east-west extension regionally and up to 100% locally.

Wright (1976) indicates the province may be subdivided into two deformation fields (Figure 5). The first field has deformation resulting from generally northwest-southeast extension with the major tension axis (sigma 3) vertical, causing horsts and grabens. The second field results from the same extensional axis but the sigma 3 axis is horizontal, creating a conjugate system of strike slip faults.

Regional conjugate fault systems (Figure 6) include: (1) the Walker Lane and Fish Lake Valley-Furnace Creek right-slip fault zones of northwest trend, subparallel to the San Andreas fault zone of California; (2) many minor northeast trending left-slip faults, subparallel to the Garlock fault in southern California; and (3) the north to north-northeast trending normal slip faults that characterize block faulting

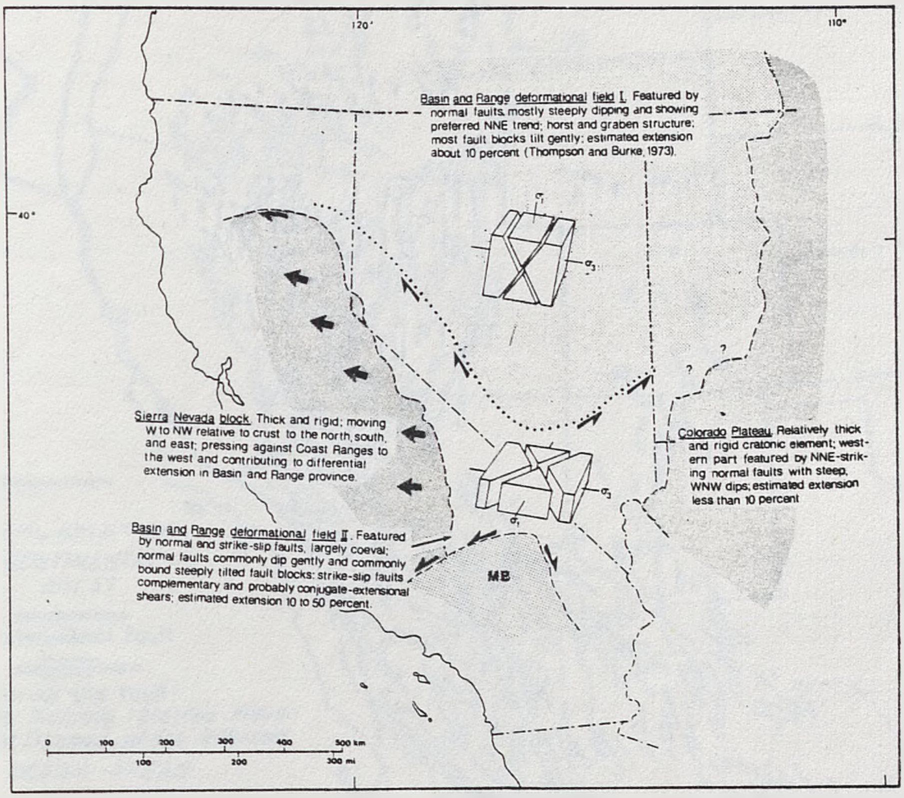

Figure 5. Tectonic model showing (1) subdivision of Great Basin into two deformation fields and (2) apparent effect of westward displacement of Sierra Nevada block and southward narrowing of Great Basin. Idealized block diagrams in each field show suggested principal stress orientations; σ_1, maximum principal stress; σ_3, minimum principal stress; MB, Mojave block (Wright, 1976).

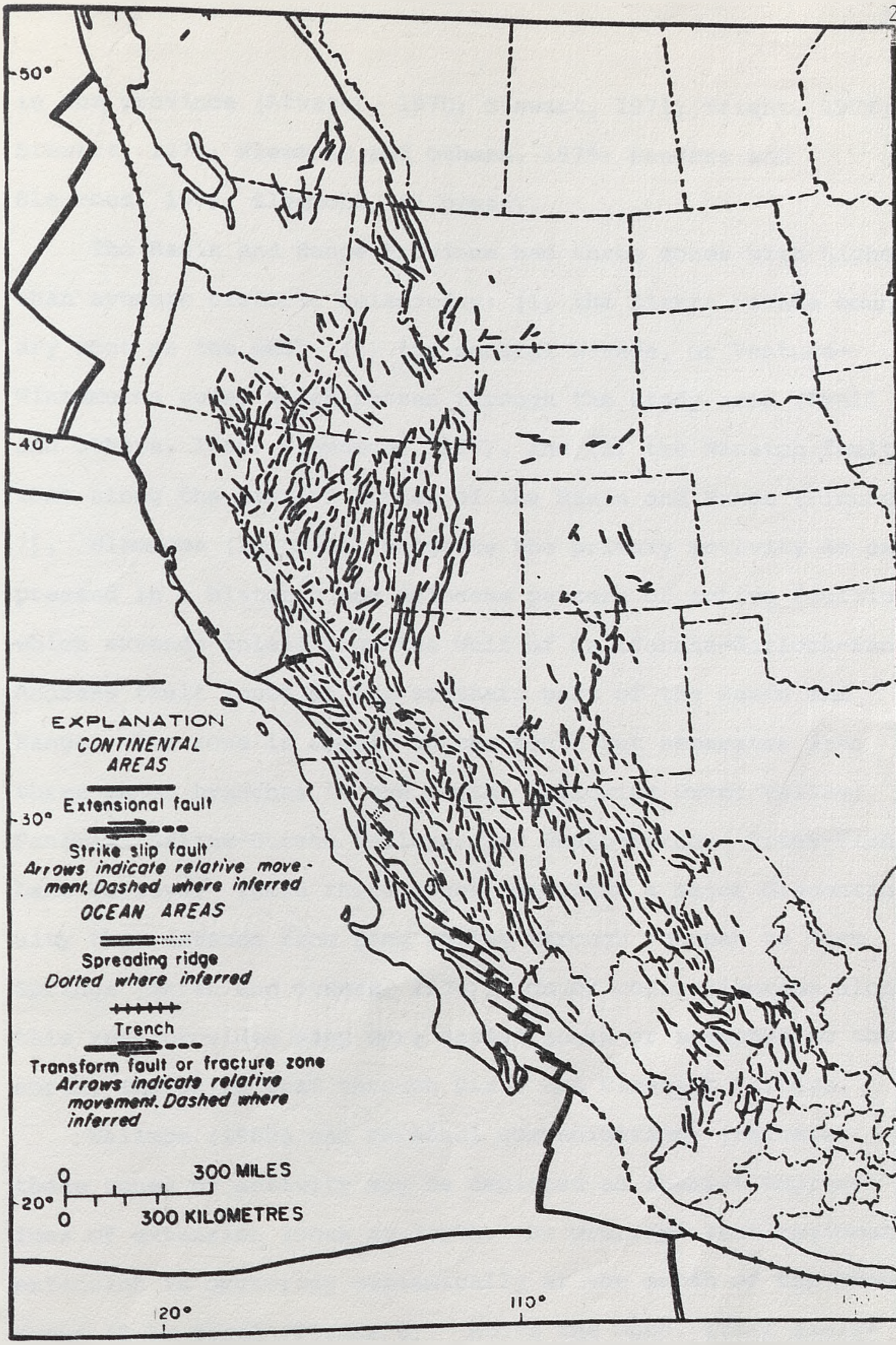

Figure 6. Major extensional faults, with some strike-slip faults in the western United States (Stewart, 1978).

in the province (Atwater, 1970; Stewart, 1971; Wright, 1976; Stewart, 1978; Slemmons and others, 1979; Sanders and Slemmons, 1979; Slemmons, in press).

The Basin and Range Province has three zones with higher than average historic seismicity: (1) the Sierra Nevada boundary zone on the west, (2) the central Nevada, or Ventura-Winnemucca zone, which passes through the study area (Ryall and others, 1966; Slemmons, 1966), and (3) the Wasatch fault zone along the eastern border of the Basin and Range (Figure 7). Slemmons (in press) suggests the primary activity is expressed in a historic and Holocene pattern of active faulting which extends inland from the Gulf of California-Garlock-San Andreas fault zones in the southern part of the Basin and Range. The zone is simple to the south but separates into three major branches to the north, following Owens Valley; Panamint-Saline-Eureka Valleys, and Death-Furnace Creek-Fish Lake Valleys. These three zones encounter a major discontinuity that extends from Long Valley through Tonopah to Warm Springs (Ekren and others, 1976). Major redistribution along this zone provides many more active zones or branches to the north, including that through Dixie and Pleasant Valleys.

Wallace (1980a and personal communication) indicates these zones of activity may be depicted as shallow expressions of extension zones at depth. He proposed that regional extension is occurring aseismically at the depth of the Moho, about 40 km depth (Figure 8). Above the Moho, still aseismically, the extension is expressed in north-south trending

Figure 7. Earthquake epicenter map for Nevada (1852-1962) for earthquakes of above about 4 magnitude with stippled pattern for zones of surface faulting (Slemmons and others, 1965).

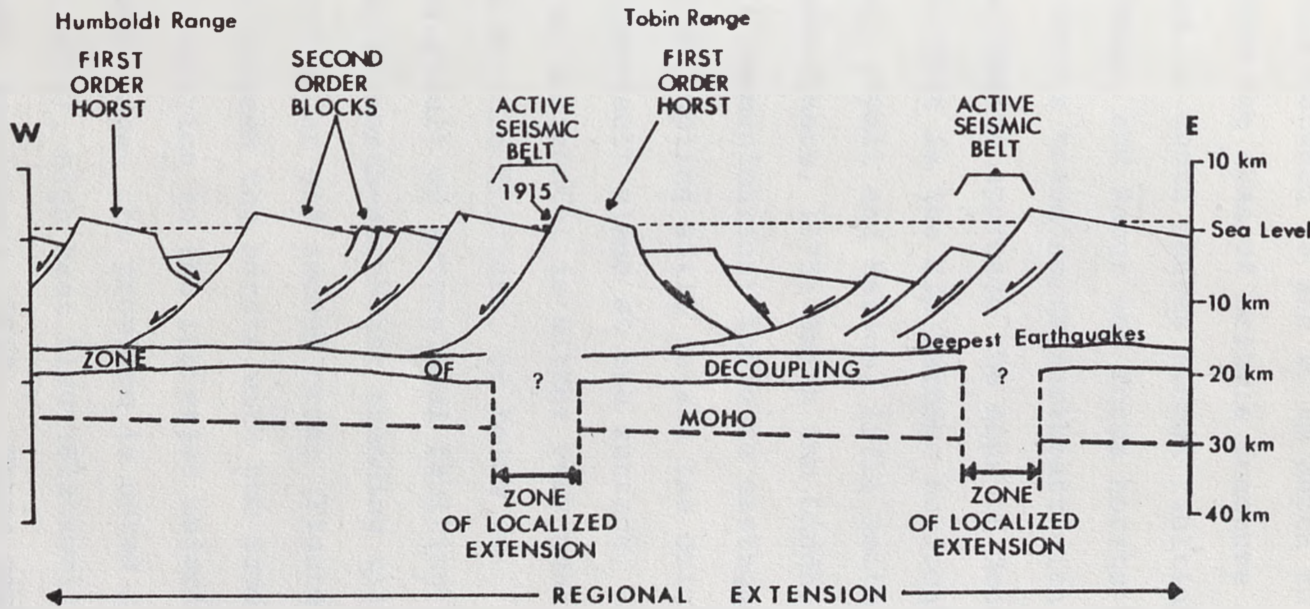

Figure 8. Diagrammatic cross section of a portion of the Basin and Range Province showing (1) eastward tilting of ranges, (2) first and second order of ranges, with some blocks representing blocks rotated and slumped off of other blocks, (3) the Moho at 30± km, (4) maximum depth of seismicity, thus of brittle zone, about 15-18 km depth, (5) narrow zones of extension at depth, (6) listric form of faults, and (7) zone of decoupling to accommodate listric-style of faulting (Wallace, 1980a).

ones of localized extension, probably accompanied by intrusion of mantle derived material. Wallace proposes a zone of decoupling between 18 and 20 km depth to accommodate extension below the area of brittle fracture in the upper crust. Extension at depth causes normal faulting in the upper crust in the Basin and Range and forms horsts and grabens. The normal faults trend north-northeast with dips of 50° - 60°. As these faults approach the zone of decoupling, they become listric, that is the dip becomes horizontal. Focal plane solutions (Ryall and Malone, 1971; Smith and Sbar, 1974; Suppe and others, 1975; Smith and Lindh, 1978; and Ryall, personal communication) indicate earthquakes at near the zone of decoupling still retain the original dip of the associated fault plane at the surface, indicating the dip change to horizontal is either very near the bottom of the zone of brittle fracture, or below it.

The result of extensional faulting in the study area is a series of north-northeast trending tilted horsts of both the first order and second order (Figure 8) and complex grabens between the horsts with the same trend.

In addition to the increased seismic activity in the Basin and Range, the province is noted by a topographic high (Smith, 1978), high heat flow (Blackwell, 1978) and a gravity low (Eaton and others, 1978). These geophysical properties of the Basin and Range are attributed to an extending lithosphere and underplating or intrusion of deeper mantle material into the upper crust (Lachenbruch and Sass, 1978).

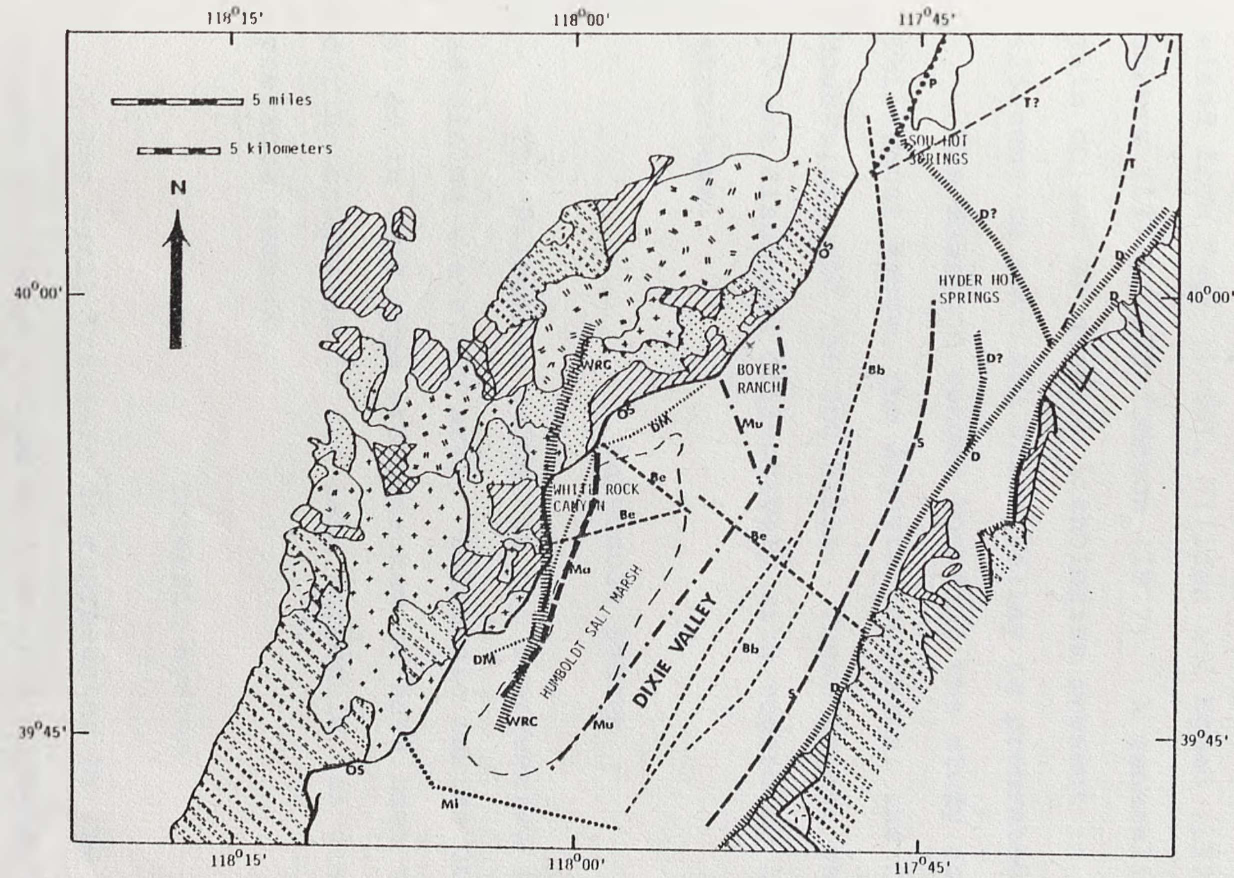

Figure 9. Generalized fault map of northern Dixie Valley, Nevada (base map from Meister, 1967). (D) Dyer fault; (OS) Old Stillwater fault; (Mu) Mud fault; (Bb) Buckbrush fault; (Be) Bernice fault; (T) Tobin fault; (P) Pleasant Valley fault; (Mi) Mississippi fault; (DM) Dixie Meadows fault; (S) Shoshone fault; (WRC) White Rock Canyon fault; (Ma) Marsh fault.

BEDROCK GEOLOGY OF ADJOINING AREA

The following discussion of the geologic units and structure in the area surrounding the study area is synthesized from Page (1965), Willden and Speed (1974), Stewart and others (1977), and Johnson (1977). A generalized stratigraphic column of bedrock lithologies present in the areas adjacent to northern Dixie Valley is presented on Plate V.

The mountain ranges bounding the study area include the Stillwater Range, the Augusta Mountains, the Clan Alpine Mountains, and the Sou Hills. These areas, shown in Plate IV are discussed collectively with regard to lithology and structure.

Paleozoic System

The Paleozoic System is not represented in the areas adjoining the study area. Paleozoic facies originally deposited in this area are presumed to have been thrust eastward during orogenies in the late Paleozoic, as discussed in the previous section.

Triassic System

The early Triassic is represented by the Koipato Group in the Stillwater, Clan Alpines, and Augusta Mountains. This group is composed of rhyolites, dacites, and greenstones locally underlain by leucogranites of early Triassic age. Overlying this group uncomformably is the Star Peak Group, consisting of the Prida and Natchez Pass Formation. These formations are present in the Stillwater Range but in the Augusta Mountains, rocks of this age are represented by the Tobin, Dixie Valley, Favret, Augusta Mountains, and Cane Spring Formations. These are in part lithologically similar, being mostly phyllite and slate with about 10% metaquartzite, carbonates and clastics, and probably represent facies changes from the Star Peak Group. In the Clan Alpine Mountains, rocks of this age are lithologically similar but have not been assigned formational names. Exposures of this sequence exceed 10,000 feet in thickness. Locally, in the Stillwater Range, an unidentified Triassic limestone is thrust over these units.

Conformably over the Star Peak Group and related rocks is the Auld Lang Syne Group, consisting of the Grass Valley, Osobb, Dun Glen, and Winnemucca Formations. All are represented in the Stillwater Range and the Osobb is present in the Augusta Mountains. In the Clan Alpines, undifferentiated rocks of similar age and lithology represent the Auld Lang Syne Group. The uppermost of this sequence may be lower Jurassic in age.

Jurassic System

Jurassic sequences are present only in the Clan Alpine Mountains and the Stillwater Range, with the exception of the top of the Auld Lang Syne Group discussed earlier. The lower Jurassic Boyer Ranch Formation is a 500 foot thick sequence of sandstone and limestone with a basal conglomerate. The upper contact is an erosional unconformity and the lower represents the Boyer thrust fault.

The Boyer Ranch Formation has been intruded by the Humboldt gabbroic complex, possibly a lopolith, composed of gabbro, diorite, and associated extrusive basalts. Age dates of 151 m.y. and 156 m.y. (Speed and Armstrong, 1971) place intrusion in the middle Jurassic. Emplacement of this complex is postulated as the driving mechanism for the Boyer thrust fault.

Upper Jurassic to Miocene Rocks

Four sequences of volcanic units and interbedded subaerial sediments from 2000 to 10,000 feet thick include acidic tuffs and breccias and basaltic andesite flows. The lower units are intruded by granitic plutons of late Cretaceous age. The episode of acidic intrusion accentuated and coarsened the metamorphic fabric of the invaded units, inducing chiastolite growth and the formation of chloritoid porphyroblasts. Locally, marble and skarn are present. Most intrusions produced contact aureoles of black hornfels or chiastolite bearing phyllite. The sequences overlie Jurassic and Triassic sediments in the Stillwater Range, the Clan Alpine, and Augusta Mountains, and outcrop as the oldest units in the Sou Hills.

Miocene Rocks

A widespread Miocene volcanic sequence, up to 4000 feet thick, includes tuffs, breccias, and flows which vary in composition from latite through rhyolite. Riehle and others (1972) have located this Miocene volcanic center in the southern Clan Alpine Mountains.

Late Cenozoic Deposits

Plio-Pleistocene to recent deposits include sediments of lacustrine and fluvial origin, locally interbedded with acidic ashes, tuffs, and flows. Pliocene to Pleistocene basalt flows, aggregated up to 1600 feet thick, are present in the lower portions of the sequence.

Structure

Stillwater Range

The Stillwater Range is a horst bounded by high-angle normal faults of large displacement. Normal faults of smaller displacement splay from the range front faults into the block.

Cenozoic rocks are folded, with increasing deformation with age. Lower Mesozoic units are highly folded and faulted. Lower Jurassic units show much deformation while the middle Jurassic units, thrust over the lower units, are much less deformed, indicating a cessation of orogeny in the lower Jurassic.

Clan Alpine Mountains

The Clan Alpine Mountains are a horst, the result of Tertiary and Quaternary block faulting. The east flank is represented by a major fault of large displacement while the west flank is marked by numerous step faults of lesser displacement. The horst block is cut by normal faults and tilted to the southeast, appearing to be part of the homocline present in the Desatoya and New Pass Ranges to the east. Folding within the Cenozoic and Mesozoic units follow that in the Stillwater Range discussed in the preceeding section.

Augusta Mountains

The Augusta Mountains, to the northeast of the Clan Alpine Mountains, are a horst bounded by large displacement normal faults. Deformation of Mesozoic units is much less severe than in the Stillwater Range and Clan Alpine Mountains, with deformation decreasing with age. This upward increase in deformation is attributed to thrusting of limestone over the Mesozoic units in the late Triassic. Cenozoic folding is also less severe than in the Stillwater Range and Clan Alpine Mountains, but attitudes follow the regional trend.

Sou Hills

Tertiary units in the Sou Hills are locally nearly undeformed but may represent a domal feature, bounded by normal faults and roughly circular in shape. The tectonic grain of the Basin and Range faulting is northeast, southwest, which is perpendicular to the main normal faults bounding the Sou Hills. No speculation of the history of this structure is offered in the literature.

ANALYTICAL RESULTS

Geomorphic Setting and Surficial Geology

A generalized geomorphic map of the study area is presented on Plate III. The area is bounded by the Stillwater Range to the northwest, the Clan Alpine and Augusta Mountains to the southeast, Jersey and Pleasant Valleys to the northeast, and the southernmost extent of the Humboldt Salt Marsh to the southwest.

Five distinct geomorphic surfaces were delineated by photogeologic interpretation (Plate III): (1) active alluvial fan surfaces, (2) inactive or highly dissected alluvial fan surfaces, (3) surfaces developed by lacustrine processes, (4) composite or undifferentiated surfaces produced by aeolian, alluvial, and lacustrine processes, and (5) the surface of the presently active playa. These surfaces represent distinct geologic and geomorphic environments (including paleo-environments) and can be correlated with distinct surficial geologic units that are assumed to be present at depth but with lateral and vertical facies changes. Boundaries between the geomorphic surface units are generally sharp with the exceptions of the facies changes between the valley fill and playa and the valley fill and active alluvial fans.

The active alluvial fans are eroded bedrock material derived from nearby mountain ranges and consist of clay-, silt-, sand-, and cobble to boulder-size material of the varying lithologies present in the mountain ranges.

Appendix A contains grain-size distribution curves for representative samples of the active fans and other surficial deposits. In general, coarser and heavier material would be preferentially deposited near the apex of a fan with finer and lighter materials being carried further down the apron (Ritter, 1979; Hooke, 1967, 1968).

The older alluvial fan deposits are similar to those of active fans, but the older surfaces are primarily undergoing degradation. These surfaces are highly dissected and surface cobbles are coated with desert varnish.

The landforms produced by lacustrine deposition include deltas, strand lines, and longshore bars. The strand lines and longshore bars are conspicuous sandy deposits and are relatively stable. They consist of well sorted cobbles, pebbles, and silt with little or no primary clay or sand. The cobbles form large patches of desert pavement and are coated with desert varnish. Carbonate cobbles on the surface exhibit flutes from aeolian processes. Locally, longshore bars have dammed post-lacustrine drainages resulting in the ponding of fine-grained (clay- and silt-size) alluvium on the upslope side. Many of these dams have been breached by more recent fluvial activity.

The composite geomorphic surfaces include valley fill deposits derived from three genetic processes. These undifferentiated deposits are predominantly silt with major amounts of clay and minor amounts of sand and gravel. This composition suggests two presently active processes with a third inactive. Active aeolian and alluvial processes are depositing predominately finer particles. The scattered sand grains are possibly aeolian with the finer silt and clay being the outwash from active alluvial fans. The occasional cobbles are assumed to be the result of flash flooding which has carried larger material beyond the active alluvial fan surfaces. Much of the silt is a result of inactive lacustrine processes and probably Lahontan in age.

The valley fill, older alluvial fans, and lacustrine deposits are all transected by active alluvial surfaces where major drainages have entrenched through these areas.

The active playa deposits are composed of fine sand, silt, and clay-sized particles and salt crystals (predominantly sodium chloride). The center of the presently active playa is marshy with active deposition of sodium chloride. The water level fluctuates and, with the extreme low relief of the playa, the surface extent of the marsh varies greatly. Surrounding the marsh is a zone of clay and silt with salt crystals emplaced by littoral action as the water level fluctuates. Three sides of the high water area are bounded by conspicuous "beach berms" which may result from the capture of aeolian material by salt cementation as salt water is carried to these areas by capillary action from the marsh and evaporated. Locally sparse vegetation is present near the perimeter of the active playa with conspicuous mounds of aeolian material, mostly silt, built up around isolated bushes. Some areas of the playa are sparsely populated by salt grasses.

Structural-Tectonic Analysis

The structural-tectonic features map (Plate II) is a composite of features delineated by photogeologic interpretation of previously available imagery and the LSA imagery generated by this study. Fault zones, interpreted from the structural-tectonic features and generalized into a single line, are shown on Figure 9 and Plate IV. Interpretation of features critical to fault delineation have been verified in the field. The fault zones delineated by surface expression correspond with subsurface structures (Figure 10) delineated by gravity, aeromagnetic, and other geophysical surveys (Meister, 1967; Smith, 1968; Stewart, 1971; Senturion Sciences, 1977, 1978; Keplinger and Associates, 1978), with the following exceptions: (1) the dip of the Old Stillwater fault is southeast, not northwest as postulated by Senturion Sciences (1977, 1978); (2) no geomorphic evidence for the Stillwater thrust delineated by Senturion Sciences (1977, 1978) was found; (3) geomorphic evidence indicates several additional faults within northern Dixie Valley including the Mississippi fault, the Dixie Meadows fault, and the Shoshone fault (Figure 9). Faults with their main expression outside northern Dixie Valley also extend into the area including the Tobin fault, the Pleasant Valley fault, and the White Rock Canyon fault (Figure 9). Following is a description of the features of the fault zones delineated on the

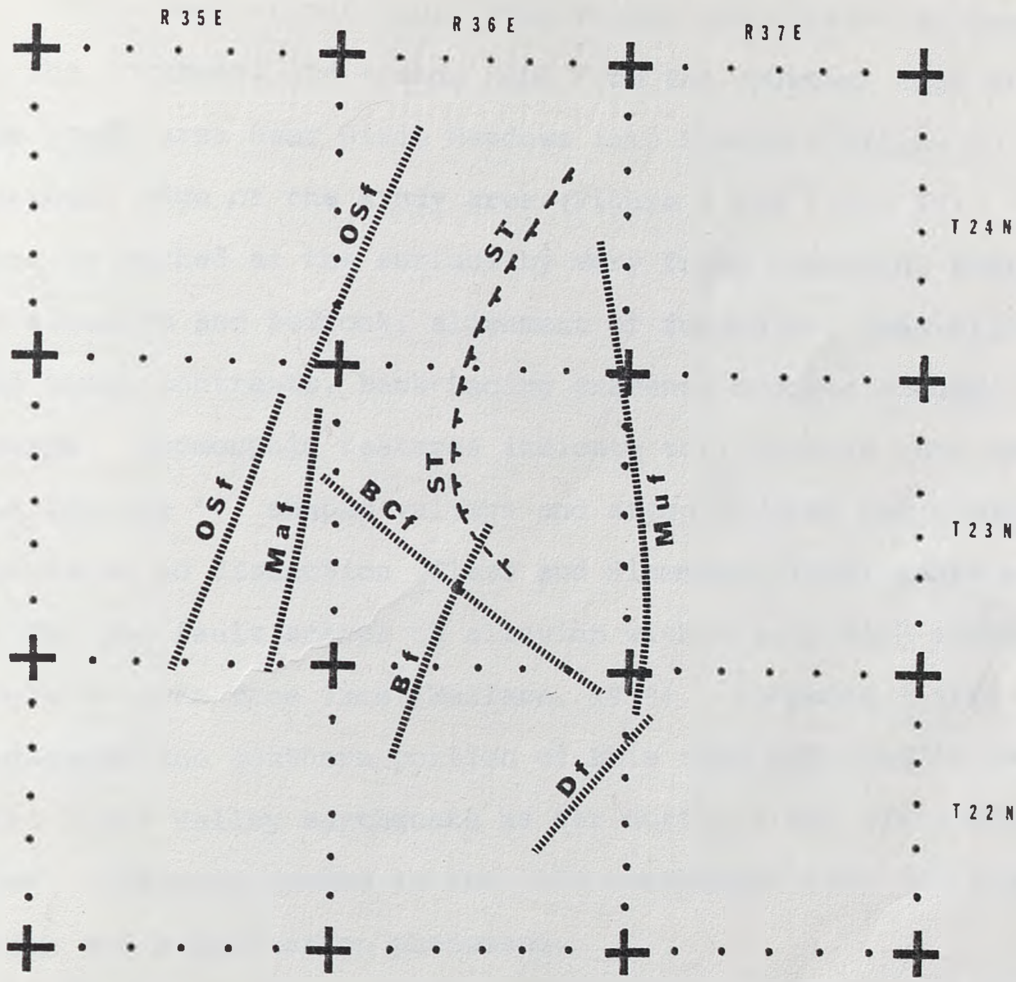

Figure 10. Diagrammatic sketch of major structural elements defined by aeromagnetic data interpretation by Senturion Sciences (1977,1978). Bf - Buckbrush fault; Df - Dyer fault; Maf - Marsh fault; Muf - Mud fault; OSf - Old Stillwater fault; ST - Stillwater Thrust fault (?); BCf - Bernice Creek fault.

structural-tectonic map.

Old Stillwater fault

This range-front fault zone bounds the Stillwater Range to the southeast and trends N36E from the southern edge of the study area near Dixie Meadows into Pleasant Valley on the northern edge of the study area (Figure 9 and Plate IV). The zone is marked at the surface by very fresh appearing scarps in alluvium and bedrock, alignment of fumaroles, vegetation, and tonal contrasts, back-facing grabens, breccia slumps, and slumps. Geomorphic features indicate this zone is very active and include 'V' shaped valleys and steep faceted spurs with little or no dissection (Glass and Slemmons, 1978; Wallace, 1978a) and fault scarps in alluvium with a very high slope angle or even free face (Wallace, 1979). Slemmons (1966) indicates the southern portion of this zone ruptured in the 1954 Dixie Valley earthquake as far north as the Dixie Meadows. Features formed in the 1954 earthquake near the Boyer Ranch are liquefaction phenomena.

Field measurements of a southeast dip of 50 to 60 degrees for this zone are consistent with the literature (Slemmons, 1957a; Larson, 1957; Page, 1965; Burke, 1967; Meister, 1967; Ryall and Malone, 1971; Stewart, 1971). Site-specific evidence for the southeast dip includes: (1) measurable fault planes on bedrock surfaces, (2) surficial geomorphic expression of normal faulting including back-facing grabens, and (3) fault plane solutions for a N55W tensional (Sigma 1) direction in northern Dixie Valley (Ryall and Malone, 1971). First order Riedel shears (Tchalenko, 1970) indicate the fault zone has a minor right-slip component. Regional studies also indicate extension of the study area in a general N55W direction (Thompson and Burke, 1973; Wright, 1976). These data are incompatible with the interpretation of aeromagnetic data by Senturion Sciences (1977, 1978) indicating a N55W dip for this zone.

The maximum elevation of the Stillwater Range to the northwest of the fault zone is greater than 7200 feet and alluvial fill in the valley to the southeast of the fault zone is nearly 2000 feet below the present valley elevation of about 3100 feet indicating greater than 6000 feet total vertical separation along this zone.

Studies of fault scarp morphology along this zone show the scarp was formed by a single movement averaging 3 meters of vertical separation (Appendix B, profiles 1-5). The section of this fault from Dixie Meadows to Sou Hills is defined as a seismic gap (Wallace, 1978b). Along the length of the seismic gap, scarp height varies from 0 to 3 meters seen at White Rock Canyon. In those areas where the scarp exceeds 1 meter in height, slope angles of 26°-30° are present. Using the slope-angle-scarp age relationships of Wallace (Figure 11), the slope angles present indicate an age of 1000 to 5000 years for the last surface faulting on this zone. Wallace (1977 and personal communication) and Bucknam and Anderson (1979) indicate caution must be exercised in not using

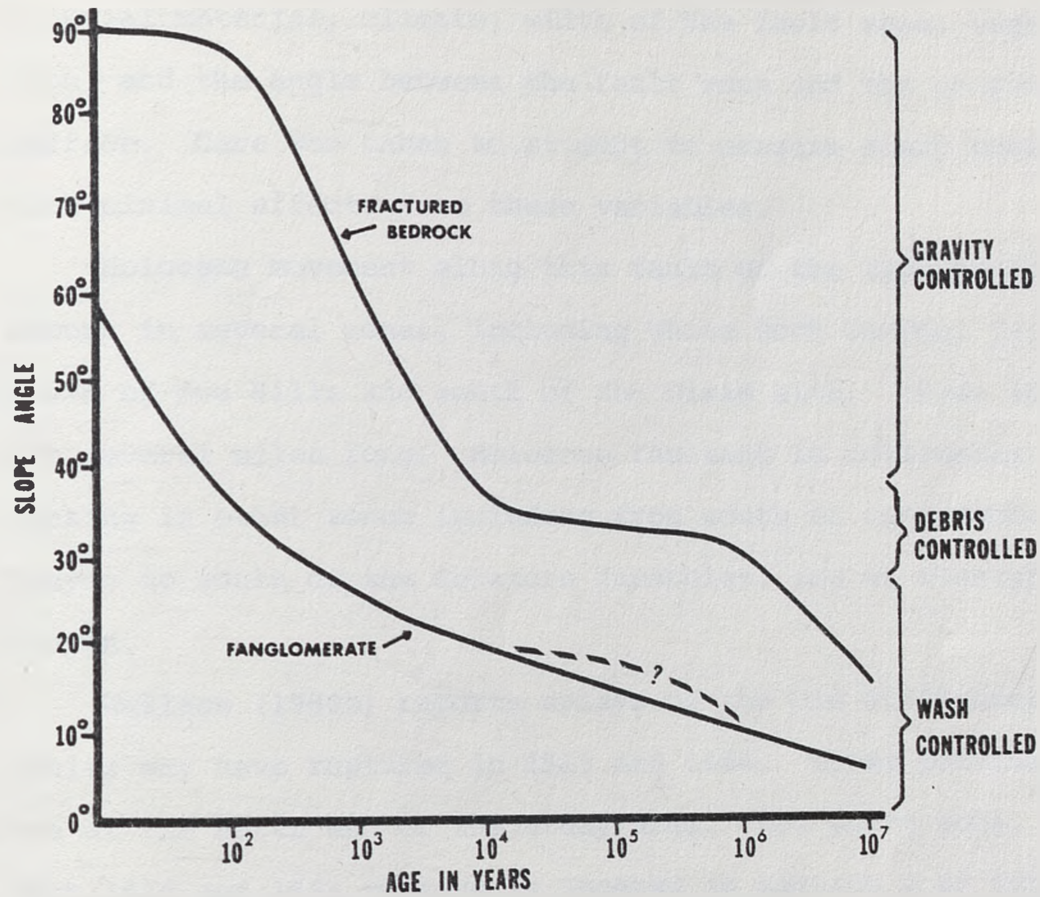

Figure 11. Limits of principal slope angle versus age of fault scarp (Wallace, 1977).

measurements from scarps that are below 1 meter or above a few meters in height as scarp degradation is dependent on scarp height. Also affecting degradation rates are type of alluvial material, climate, width of the fault zone, vegetation, and the angle between the fault zone and the original surface. Care was taken to attempt to measure scarp profiles with minimal effects from these variables.

Holocene movement along this fault of the type profiled occurs in several zones, including White Rock Canyon, just south of Sou Hills and south of the Dixie site. These zones are several miles long. Holocene faulting is noticeably lacking in other zones including from south of Cottonwood Canyon to south of the Senators fumaroles, and at Mississippi Canyon.

Wallace (1980b) reports splays of the Old Stillwater faults may have ruptured in 1915 and 1954. These portions are at the north end of the study area. One short zone, with both 1915 and 1954 rupture is located in Section 8 of T25N, R37E, and is within the Stillwater Range. This scarp may represent block slumping rather than tectonic faulting, however (Wallace, 1980b).

Marsh fault

The Marsh fault extends from the southern edge of the study area along a N30E trend to its intersection with the Old Stillwater fault in Section 36, T24N, R35E, (Figure 9 and Plate IV). The surface expression, although somewhat subdued along the northwest edge of the Humboldt Salt Marsh, is marked by stream and vegetation alignments, subtle scarps and grabens. Scarps preserved in Sections 6 and 7, T23N, R35E, and Sections 10 and 16, T22N, R35E, indicate normal faulting with the southeast block downdropped. This is compatible with aeromagnetic interpretations (Senturion Sciences, 1977, 1978).

Buckbrush fault

The Buckbrush fault is a semi-arcuate fault concave to the southwest trending N30E from the southern edge of the study area to the Bernice fault when it splays into two branches (Figure 9 and Plate IV). Both splays intersect the Old Stillwater fault, the western splay in Section 4, T24N, R36E, and the eastern splay near the Senator fumaroles in Sections 28 and 29, T25N, R37E. Surface expression is marked by subtle scarps, spring and vegetation alignments, and vegetation and tonal contrasts. The northwest block is downdropped in the southern portion of the zone but relative movement is not discernible in the northern portion.

Mud fault

The Mud fault trends N36E from the Dixie Settlement area to Section 4, T23N, R35E, then follows a N15E trend to Sou Hills (Figure 9 and Plate IV). Surface expression of the southern portion indicates the northwest block is downdropped. Near Sou Hills several interpretations are possible: (1) the fault joins the frontal fault system on the east side of

Pleasant Valley (Pleasant Valley fault), (2) the fault joins the Old Stillwater fault system and continues along the west side of Pleasant Valley, or (3) the fault is related to the frontal fault system on the east side of the Tobin Range (Tobin fault).

A southeast splay of this fault, mapped by Senturion Sciences (1977, 1978) as the Mud fault (Figure 10), shows surface expression as moderate scarps near the mouth of Deep Canyon and trends N25E to intersection with the main zone is Section 30, T23N, R37E. However, this splay could be related to the Shoshone fault with the Mud fault being a separate and distinct structure. In either interpretation, the block northwest of this splay is downdropped.

Dyer fault

The Dyer fault transects the study area along a N36E trend from the mouth of Meadow Spring Canyon on the south and is the frontal fault of the Clan Alpine and Augusta Mountains (Figure 9 and Plate IV). The northwest block is downdropped along this zone. A splay of this fault appears to arc across Dixie Valley just north of Hole-in-the-Wall and join the frontal fault system on the west side of the Tobin Range in Pleasant Valley (Pleasant Valley fault).

The Clan Alpine Mountains reach a height in excess of 8000 feet, with alluvial fill of unknown thickness below the 3600 feet mean elevation valley floor, which indicates greater than 5000 feet total vertical separation along this zone.

Examination of scarps on this zone show angles of 9° to 12° near the mouth at Shoshone Creek. Wallace's (1977) dating of the scarps at Shoshone Creek would be 9000 to 15,000 years (Figure 11). Segments of this zone show similar movement elsewhere but some segments are not marked by scarps, showing inactivity for several hundred thousand years (Wallace, 1977).

Bernice fault

The Bernice fault (Bernice Creek fault of Senturion Sciences, Figure 10) is a main crosscutting feature in northern Dixie Valley. Surface expression of vegetation and tonal contrasts and stream and spring alignments indicate the zone extends along an arcuate trace northwest from Bob Canyon toward the Dixie site in the Stillwater Range (Figure 9 and Plate IV). A splay of this zone may arc to the north and join the Marsh fault near Section 17, T23N, R36E. Surficial geomorphic deposits indicate the southwest block is downdropped as the lowest area of the valley floor, the Humboldt Salt Marsh, is immediately southwest of the fault trace. However, bedrock geology near the Dixie site indicates the northeast block may be downdropped, as does aeromagnetic data (Senturion Sciences, 1977, 1978). Surface expression is subtle and relative movement on the zone is not discernible from surface evidence.

Stillwater thrust

Senturion Sciences (1977, 1978) postulated this structure in the alluvial fill in the center of Dixie Valley area based on interpretation of aeromagnetic data (Figure 10). As thrusting in alluvium filled valleys in the Basin and Range is rare and no geomorphic features of thrusting are discernible, the existence of this structure is questionable.

Mississippi fault

Another fault zone (Mississippi fault) extends across Dixie Valley along a S40E trend from the mouth of Mississippi Canyon, crosscutting the valley (Figure 9 and Plate IV). Surface expression includes low scarps, vegetation and tonal contrasts, and stream alignments. These features are subtle but indicate the southwest block is downdropped. Surficial geomorphic deposits indicate the opposite may be true as the Humboldt Salt Marsh lies immediately northeast of this zone.

Dixie Meadows fault A

A major fault zone (Dixie Meadows fault) trends N36E from the southern edge of the study area across Dixie Meadows, subparallel to and between the Old Stillwater and Marsh faults (Figure 9 and Plate IV). This Dixie Meadows fault corresponds to the valley branch splay of the Stillwater Range frontal fault of Trexler and others (1978). The zone continues in an arcuate path concave to the northwest and merges with the Old Stillwater fault in Sections 35 and 36, T24N, R35E. The southwest block is downdropped as evidenced by numerous slumps, asymmetric grabens, and southeast facing scarps. Spring and vegetation alignments are also present. Liquefaction phenomena, including slumps and sand boils, are present along the portions of this fault that lie near highly saturated playa deposits.

Slemmons (1957a) has mapped surface rupture on this zone during the 1954 Dixie Valley-Fairview Peak earthquake in Dixie Meadows. Examination of the 1954 rupture shows that it is entirely in valley fill deposits, not alluvium (Plate III) and scarp morphology studies using Wallace's (1978a) plot of data are not appropriate for this type of surface material.

Shoshone fault

A fault (the Shoshone fault) northwest of and subparallel to the Dyer fault trends N30E with maximum surface expression near the mouth of Shoshone Creek (Figure 9 and Plate IV). In addition to vegetation contrasts, surface expression is marked by scarps which indicate the block to the northwest is downdropped. Hyder Hot Springs may be associated with this structure.

Investigation of scarps associated with this zone in valley fill deposits show low slopes (7^{o} - 10^{o}) but the zone offsets longshore bars and delta deposits and scarps are present below the Lahontan age shorelines. This indicates movement in portions, if not all of the zone, in Holocene times.

Pleasant Valley fault

The Pleasant Valley fault is the frontal fault system on the west side of the Tobin Range (Figure 9 and Plate IV).

The fault zone is wide but activity in 1915 created a very sharp southwest facing scarp from surface rupture near the bedrock-alluvium contact (Slemmons, 1966). Wallace (1980b) has mapped 1915 movements within the north edge of the study area in Sou Hills. This zone crosses the Sou Hills to the southwest and apparently ends in the northern portion of Dixie Valley.

Tobin fault

The frontal zone on the east side of the Tobin Range (Tobin fault) extends southwest into the study area and apparently dies out in the north end of Dixie Valley (Figure 9 and Plate IV). A splay of this fault may cross to the southeast of Sou Hills and merge with the Old Stillwater fault. Scarps along this zone indicate the southeast block is downdropped. Sou and Seven Devils Hot Springs are associated with this structure.

A fault scarp profile on this scarp (Appendix B, profile 6) indicates 3 displacements dated by Wallace's methods (1977) as less than 10,000 years old. Displacements range from 1 m to 3 m. This profile, compared to those on the Old Stillwater fault, indicates a separate tectonic regime for this fault as only one Holocene movement is discernible on the Old Stillwater fault, while 3 are shown at this location.

White Rock Canyon fault

A fault (White Rock Canyon fault) traces diagonally north-south across the Stillwater Range, following White

Rock Canyon in the study area (Figure 9 and Plate IV). This fault joins the Old Stillwater fault immediately southwest of the mouth of White Rock Canyon and trends south, splaying south from the Old Stillwater fault in Section 23 of T23N, R35E. Surface expression for this zone includes vegetation and tonal contrasts and lineations in Dixie Valley, displaced bedrock in White Rock Canyon and, regionally, the apparent left-lateral displacement (Figure 12) of the Humboldt gabbroic complex (Humboldt lopolith of Speed, 1976).

The displacement shown on the Humboldt gabbroic complex contrasts with that proposed by Smith (1968). From aeromagnetic data, including a standard aeromagnetic map of Dixie Valley showing the residual magnetism of the area and the second vertical derivative of the data to show the rate of change of the residual magnetism of the area, Smith (1968) interpreted about 1 mile of right-lateral displacement of the eastern portion of the gabbroic complex on what corresponds to the Buckbrush fault in this report. A review of this data indicates a noticeable anomaly which Smith interpreted as the southern edge of the gabbroic complex beneath alluvium in Dixie Valley. This anomaly may instead correspond to a downdropped southwest block on the Mississippi fault. Another anomaly crossing the valley about 11 miles to the northeast may represent the southern boundary of the Humboldt complex in Dixie Valley (Figures 13 and 14). This interpretation is consistent with outcrops of the gabbroic complex in the Clan Alpine Mountains and Stillwater Range

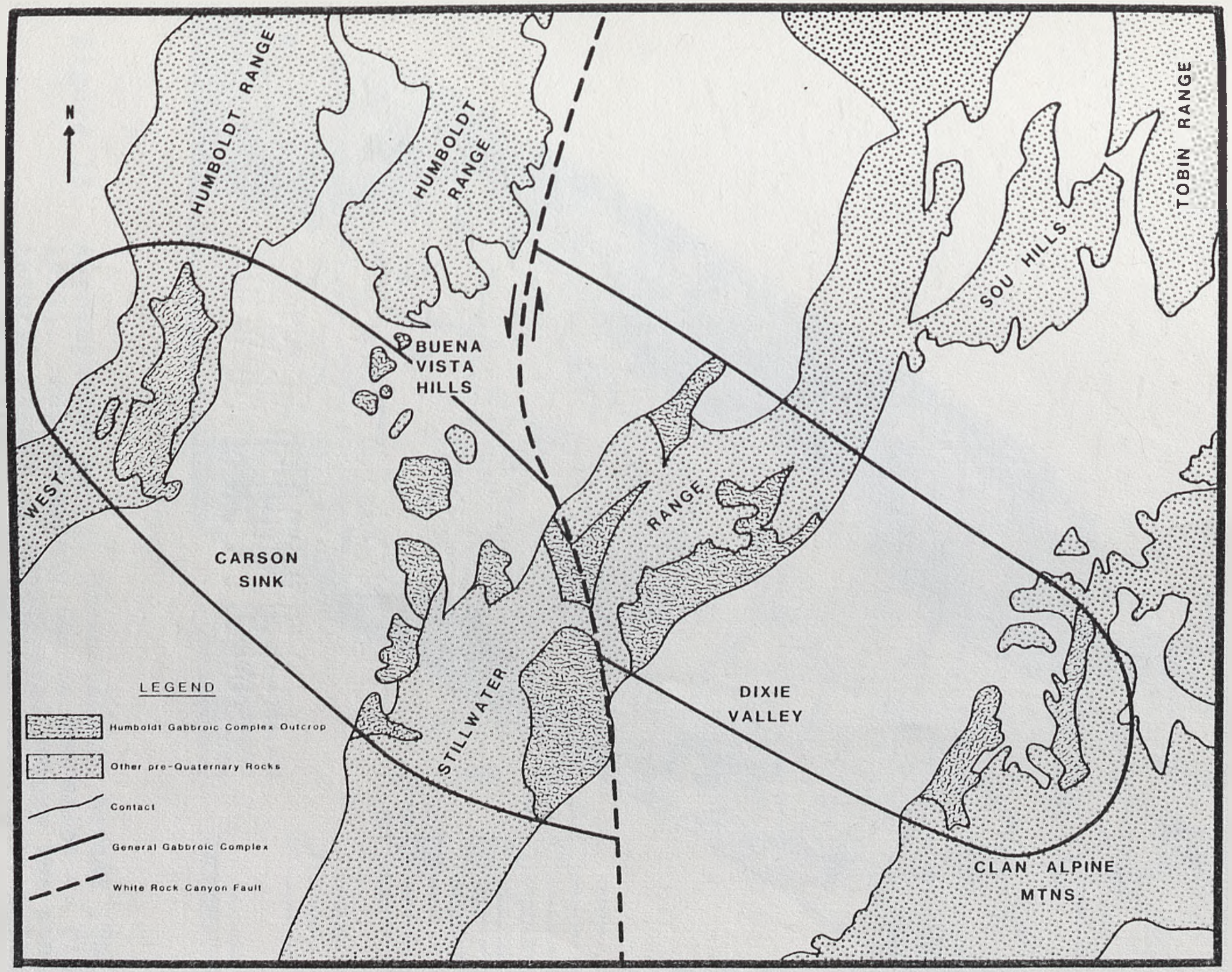

Figure 12. Generalized geologic map showing extent of the Humboldt gabbroic complex (Humboldt Lopolith of Speed, 1976).

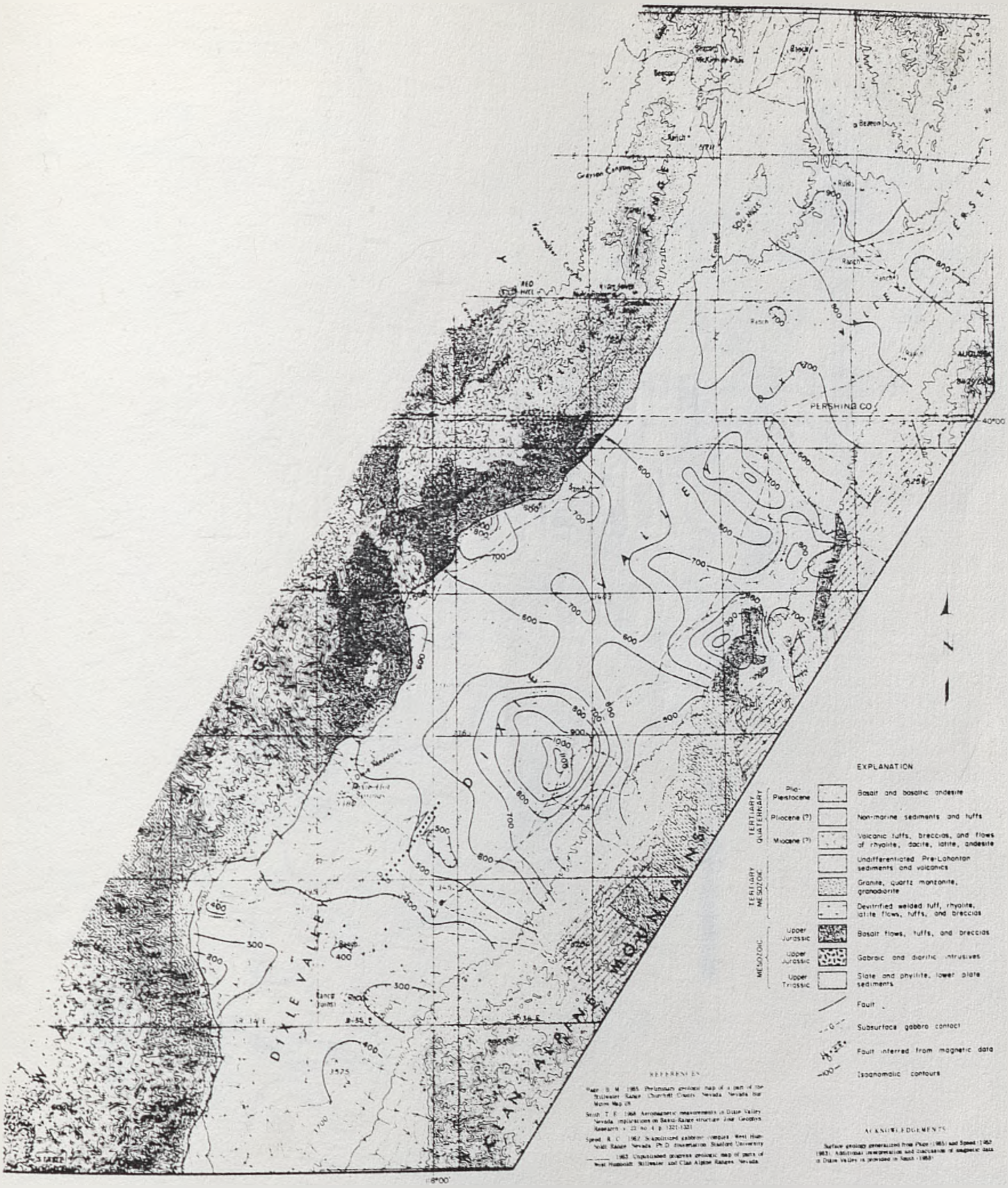

Figure 13. Aeromagnetic map of Dixie Valley, Nevada (Smith, 1971). Approximately one to two miles of right-lateral offset is interpreted across the southern boundary of the gabbroic complex by Smith.

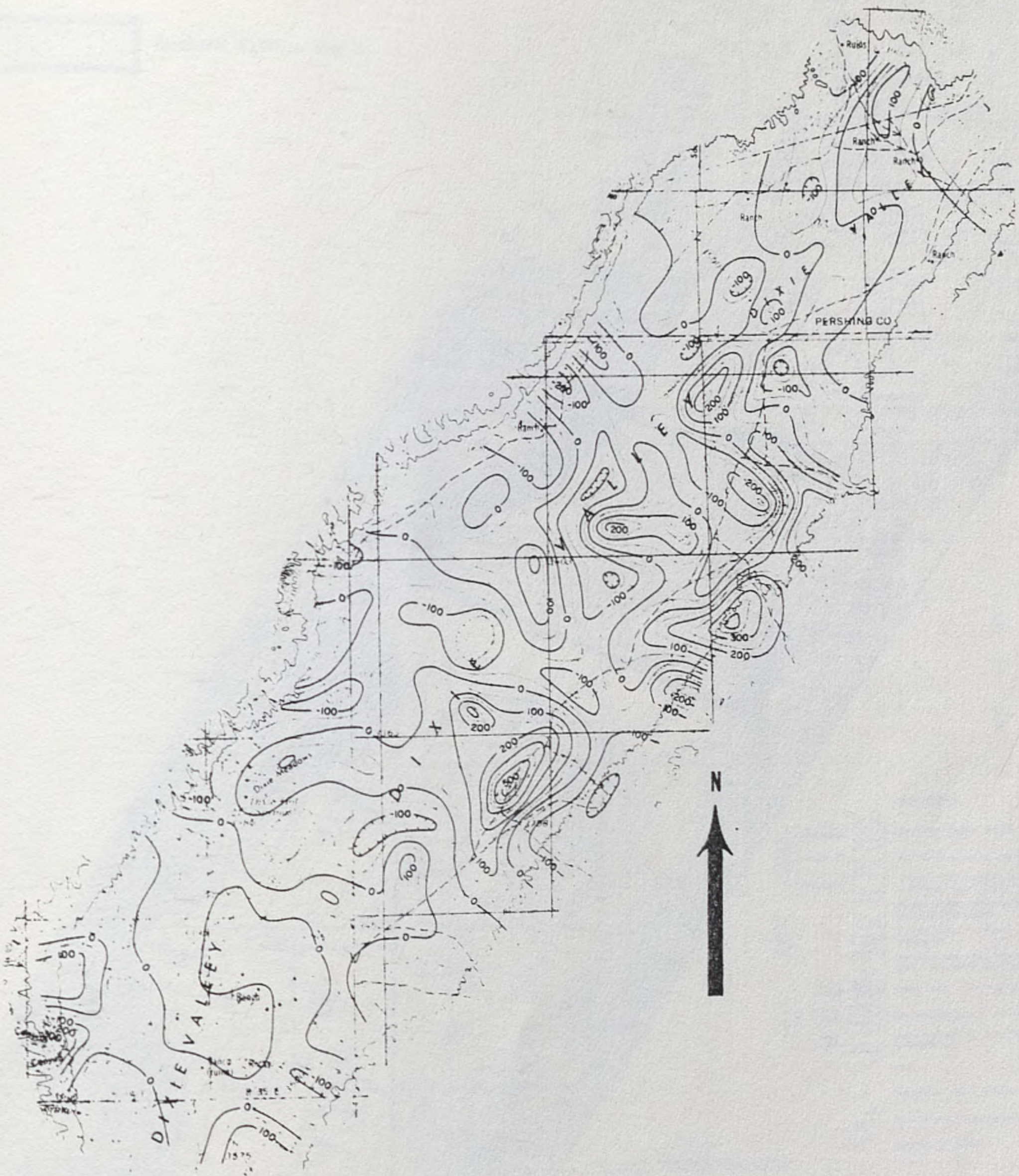

Figure 14. Second vertical derivative of aeromagnetic data for Dixie Valley, Nevada (Smith, 1971).

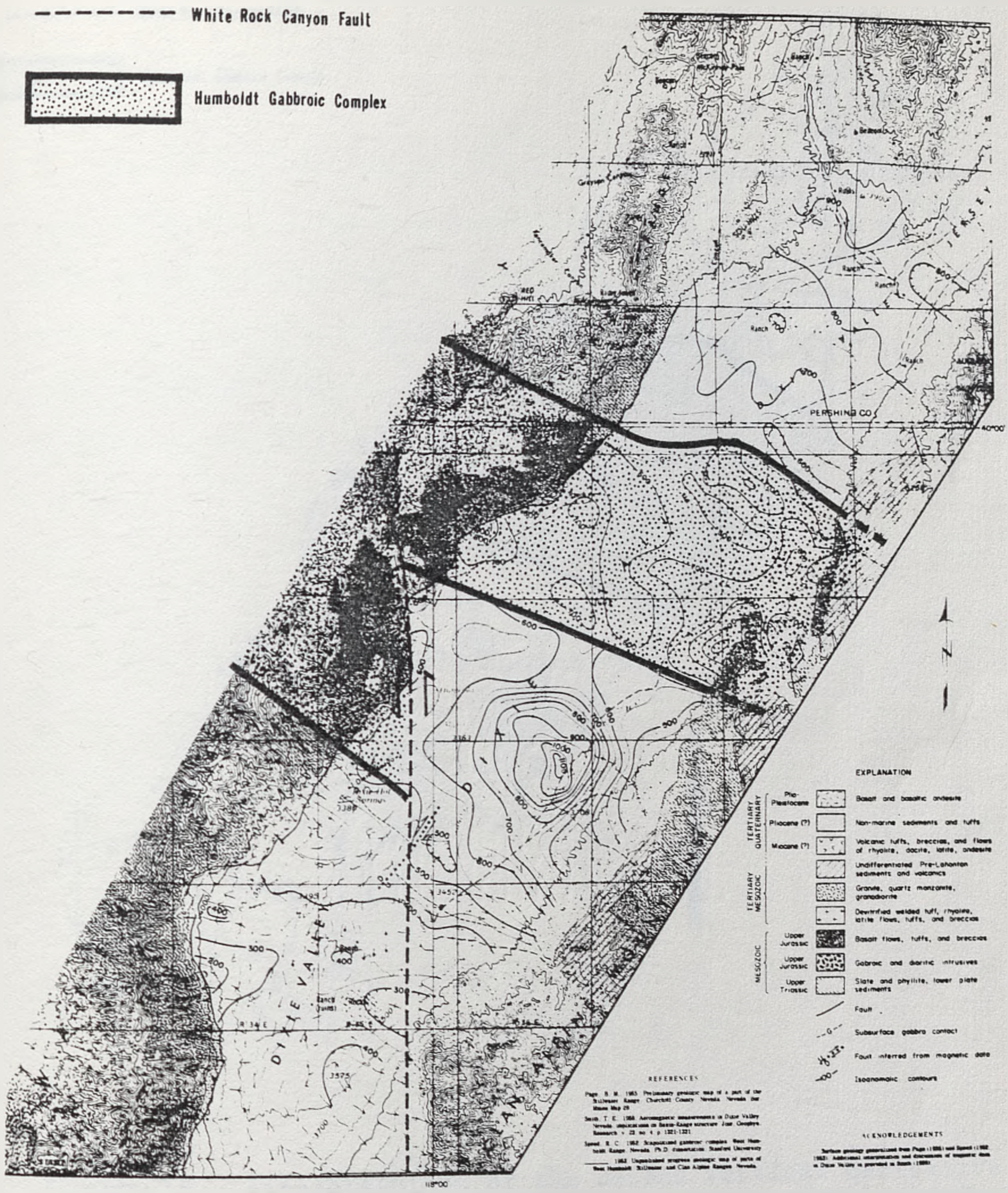

Figure 15. Re-interpretation of aeromagnetic map of Dixie Valley showing the left-lateral White Rock Canyon fault and the proposed boundaries of the Humboldt gabbroic complex (aeromagnetic data from Smith, 1971).

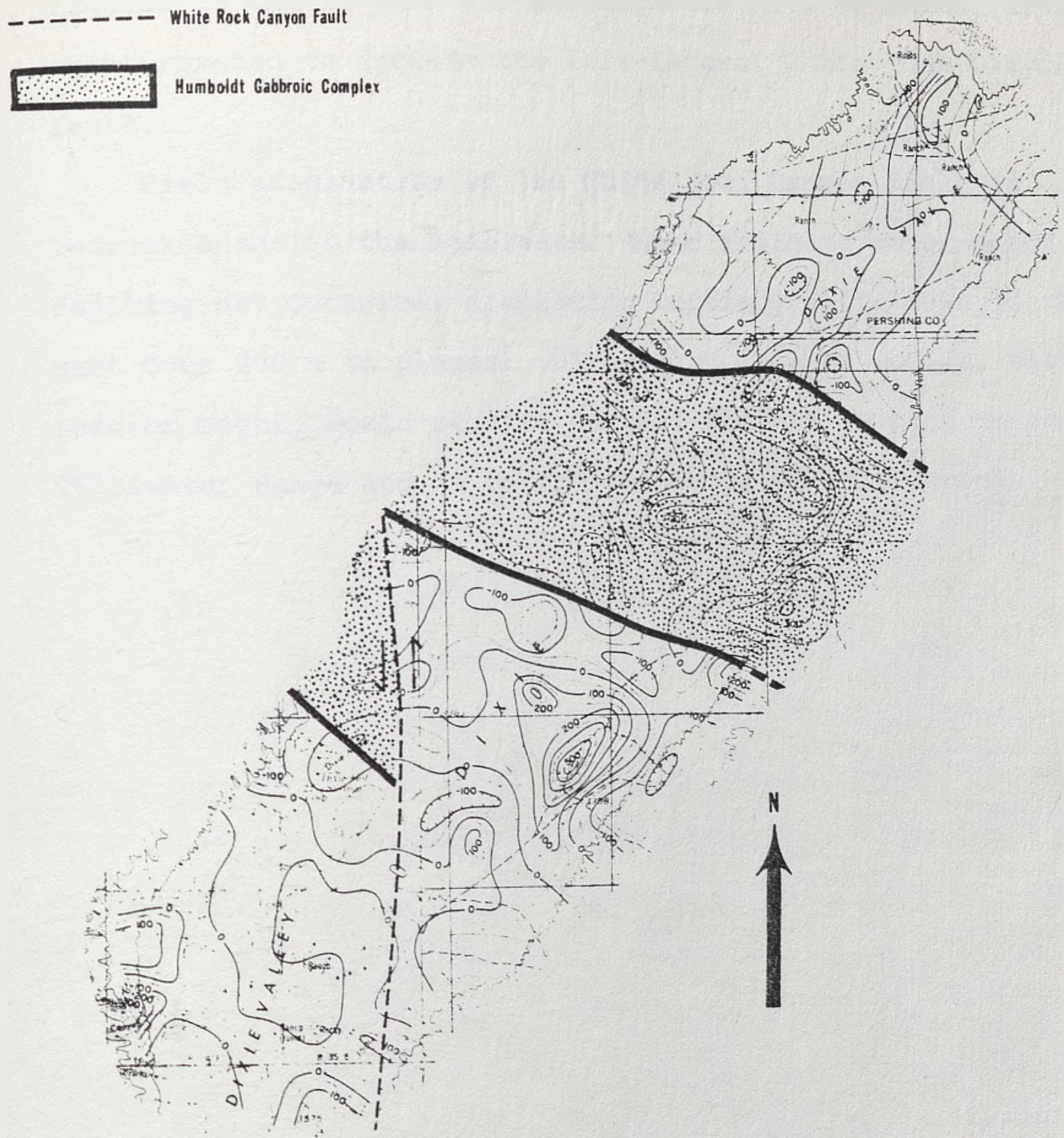

Figure 16. Interpretation of the second vertical derivative of the aeromagnetic data of Smith (1971) showing the left-lateral White Rock Canyon fault and the proposed boundaries of the Humboldt gabbroic complex.

Figures 15 and 16 show the aeromagnetic data of Smith (1968) reinterpreted to include the left-lateral White Rock Canyon fault.

Field examination of the White Rock Canyon fault in bedrock areas in the Stillwater Range indicate major normal faulting has occurred, displacing Tertiary tuffs down to the east over 300 m in places. Discerning lateral motion, either left or right, would require careful bedrock mapping in the Stillwater Range and is beyond the scope of this report.

INTERPRETATIONS AND CONCLUSIONS

Geomorphic Surfaces

A distinct relationship is seen between the geographic position of geomorphic surfaces and the structural-tectonic features in Dixie Valley. In the most obvious of these relationships, the active playa surface and the Humboldt Salt Marsh are bounded on all four sides by structural features (Figure 9 and Plate IV). On the northwest side of the active playa, the Marsh fault marks the boundary zone with alluvial fan deposits while to the southeast, the boundary with valley fill is marked by the Buckbrush fault. The boundary on the northeast extends over the Bernice fault and corresponds generally with a splay of the Buckbrush fault where it transects the valley. The southwest edge of the playa corresponds with the Mississippi fault. The two crosscutting features of Dixie Valley, the Mississippi and Bernice faults, define the boundaries of the Humboldt Salt Marsh. These studies place an active inner-graben to the northwest of the longitudinal axis of Dixie Valley and the salt marsh, and active playa surfaces are displaced in the same manner with respect to the longitudinal axis.

The alluvial, lacustrine, and aeolian deposits included in the undifferentiated valley fill are located northeast and southwest of the active playa surface. These sediments extend northward into both Pleasant and Jersey valleys, and southward in Dixie Valley beyond the study area. Like the playa deposits, these sediments are shifted northwest of the longitudinal valley axis.

Active alluvial fan surfaces extend from bedrock on both sides of the valley to the playa or valley fill deposits. These deposits are asymmetrically distributed as a narrow band (up to 2 1/2 miles wide) of steeply sloping fan surfaces extending southeast from the Stillwater Range, and a wide band (3 to 7 miles wide) of gently sloping surfaces extending northwest from the Clan Alpine and Augusta Mountains. A third narrow band encircles the southern end of the Tobin Range. The wider band of coalesced fan surfaces (bajada) on the east side of the valley are embayed deeply into the source mountain ranges but those on the west side extend only a short distance into canyons of the Stillwater Range.

The older alluvial deposits are nearly absent on the western, more active side of the valley but are more common to the north and east where they generally adjoin bedrock.

The lacustrine deposits, including deltas, strand lines, and longshore bars, are predominantly near the playa and some distance from bedrock on the eastern and northern portions of the valley where they overlie alluvium and valley fill deposits. The scattered small deltas on the west side of the valley overlie fan surfaces only and generally adjoin bedrock. This assymetric distribution of all geomorphic surfaces indicate a faster rate of subsidence on the northwest side of the valley.

Structural-Tectonic Model

A three dimensional model of the northern portion of Dixie Valley depicts the structural relationships among the various tectonic elements, with the alluvium removed and the bedrock or basement surface restored (Figure 17). This modified interpretation incorporates all fault zones described in this report with the exception of the postulated Stillwater thrust fault (Senturion Sciences, 1977, 1978). Although the relative movement on the Bernice and Mississippi faults is uncertain, a downthrown southwestern block is depicted in the model.

A mechanism for the formation of graben valleys similar to Dixie Valley is reviewed by Stewart (1971). Tchalenko (1970) and Cloos (1955, 1968) have assumed laboratory clay models of fault and/or deformation systems mimic geological systems. A model developed by Cloos (1968) for Basin and Range horst and graben formation (Figure 18) closely resembles the three dimensional model presented in Figure 17 for Dixie Valley. Wallace (1980) suggests regional decollement at depth (Figure 8) which is compatible with Cloos' (1968) model. Ryall (personal communication) cites the lack of deep seismicity in the Basin and Range as evidence for decollement at about 20 km depth.

The longitudinal asymmetry of Dixie Valley also fits well with laboratory models developed by Cloos (1968). The downdropping of one side of the graben in the model

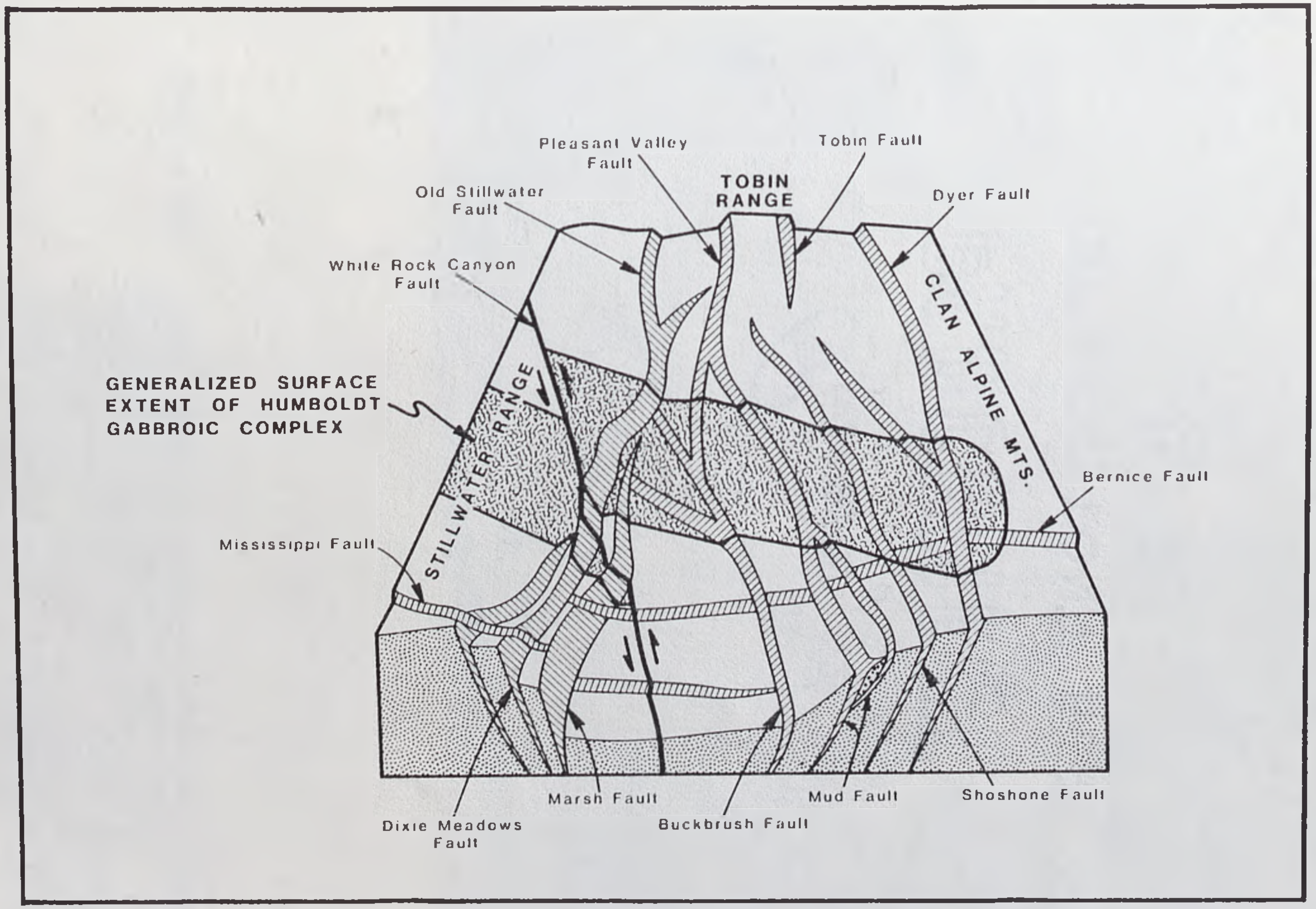

Figure 17. Three dimensional model of the northern portion of Dixie Valley, Nevada. The structural relationships among the various tectonic elements are depicted, with alluvium removed and the bedrock or basement surface restored (modified from Smith, 1967).

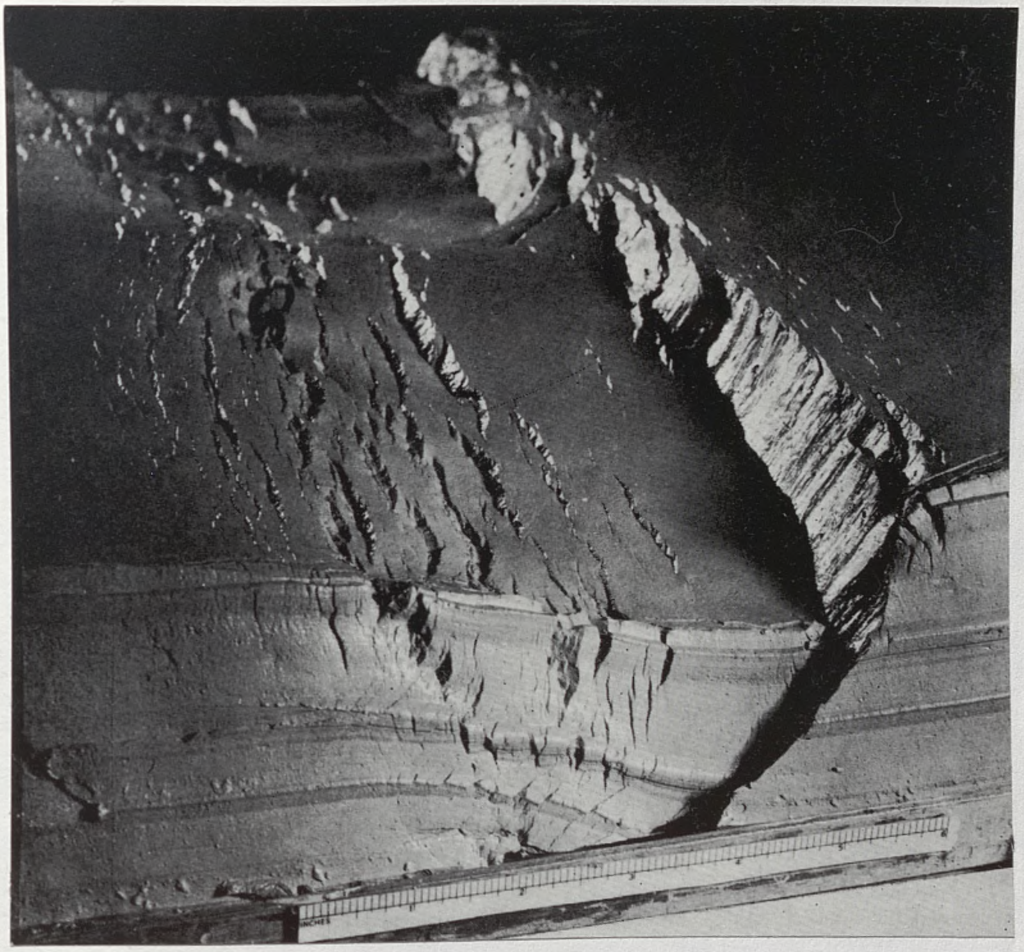

Figure 18. Clay model of graben formation showing asymmetry of the bounding faults. Note arcuate cross-cutting structure. Right block moved right; left block remained stationary. Reprinted from Cloos (1968) with permission of the American Association of Petroleum Geologists.

corresponds with the structural interpretation along the Stillwater margin of the valley. Slump block faulting of the model closely resembles interpretation along the Clan Alpine and Augusta Mountains. A distinct arcuate crosscutting feature developed in the model may correlate with the arcuate crosscutting splays of the Buckbrush and Dyer faults.

The graben model postulated above would suggest more active (i.e., greater amounts of) subsidence in a zone along the western side of the valley. Alluvial fans (and other deposits) in this zone would tend to be covered more rapidly by playa deposition on this downdropping block. Conversely, older alluvial fans, older delta deposits, and a much wider zone of active alluvial deposition would be expected on the surface of the more brecciated side of the graben where the total displacement is distributed across a series of step faults. This is consistent with the distribution of the various geomorphic surfaces within northern Dixie Valley (Plates III and IV).

The above model does not explain crosscutting features which extend into bedrock such as the Mississippi, Bernice, and White Rock Canyon faults. These are inferred to be older faults which predate the inception of Basin and Range faulting (15 to 17 m.y. ago; Stewart, 1971) but are still active, affected by Basin and Range tectonics because their attitudes are near those of normal faulting under the present regional strain patterns. Geomorphic features along these fault zones include subtle scarps, spring alignments and vegetation contrasts indicating late Quaternary, possibly Recent, movement.

Gravity data (Stewart, 1971; Erwin and Bittleston, 1977; Erwin and Berg, 1977) are consistent with the model of a complex asymmetric graben. Structural relationships defined by aeromagnetic surveys (Smith, 1971; Nevada Bureau of Mines and Geology, 1977; Senturion Sciences, 1977, 1978) are in close agreement with clay model experimental data (Cloos, 1955, 1968) and the structural-tectonic features delineated by surficial expression in Dixie Valley (Plate II).

REFERENCES

Atwater, T., 1970, Implications of plate tectonics for the Cenozoic tectonic evolution of western North America: Geol. Soc. America Bull., v. 81, p. 3513-3536.

Blackwell, D.D., 1978, Heat flow and energy loss in the western United States; in Smith, R.B., and Eaton, G.P., eds., Cenozoic tectonics and regional geophysics of the western Cordillera: The Geological Soc. of America Memoir 152, p. 175-208.

Bucknam, R.C., and Anderson, R.E., 1979, Estimation of fault scarp ages from a scarp height-slope-angle relationship: Geology, v. 7, p. 11-14.

Burchfiel, B.C., and Davis, G.A., 1975, Nature and controls of Cordilleran orogenesis, western United States: Extensions of an earlier synthesis, American Journal of Science, v. 275-A, p. 363-396.

Burke, D.B., 1967, Aerial photography survey of Dixie Valley, Nevada, in U.S. Air Force Cambridge Research Labs. Spec. Rept. 66-848.

Cloos, E., 1955, Experimental analysis of fracture patterns: Geol. Soc. America Bull., v. 66, p. 241-256.

Cloos, E., 1968, Experimental analysis of Gulf Coast fracture patterns: American Assoc. Pet. Geol. Bull., v. 52, no. 3, p. 420-444.

Dickinson, W.R., 1976, Sedimentary basins developed during evolution of Mesozoic-Cenozoic arc--trench system in western North America: Canadian Journal of Earth Sci. 13: p. 1268-1287.

Dickinson, W.R., 1977, Paleozoic plate tectonics and the evolution of the Cordilleran continental margin, in Stewart, J.H., Stevens, C.H., and Fritshe, A.E., eds., Paleozoic paleogeography of the western United States: Pacific section, Soc. Econ. Paleontol. and Mineral. Pacific Coast Paleogeography Symposium 1, p. 137-156.

Dickinson, W.R., 1979, Cenozoic plate tectonic setting of the Cordilleran region in the United States, in Armentrout, J.M., Cole, M.R., and Terbest, H. Jr., eds., Cenozoic paleogeography of the western United States: Pacific section, Soc. Econ. Paleontol. and Mineral. Pacific Coast Paleogeography Symposium 3, p. 1-13.

Eaton, G.P., 1979, A plate-tectonic model for late Cenozoic crustal spreading in the western United States, in Riecker, R.E., ed., Rio Grande Rift: Tectonics and magmatism. American Geophysical Union, Washington, D.C., p. 7-32.

Eaton, G.P., Wahl, R.R., Protska, H.J., Mabey, D.R., and Kleinkopf, M.D., 1978, Regional gravity and tectonic patterns: Their relation to late Cenozoic epierogenic and lateral spreading the western Cordillera: Geol. Soc. America Mem. 152, p. 51-92.

Ekren, E.B., Bucknam, R.C., Carr, W.J., Dixon, D.L., Quinlivan, D.W., 1976, East-trending structural lineaments in central Nevada, U.S.G.S. Prof. Paper 986, 16 p.

Erwin, J.W., and Berg, J.C., 1977, Bouguer gravity map of Nevada: Reno sheet: Nevada Bur. Mines and Geol., Map 58.

Erwin, J.W., and Bittleston, E.W., 1977, Bouguer gravity map of Nevada: Millett sheet: Nevada Bur. Mines and Geol., Map 53.

Exploration Data Consultants, Inc., 1976, Gravity and magnetic survey over the Humboldt Salt Marsh, Dixie Valley, Nevada: Report for Dow Chemical Company, 8 p.

✓ Glass, C.E., and Slemmons, D.B., 1978, State-of-the-art for assessing earthquake hazards in the United States, Report 11 Imagery in Earthquake Analysis: U.S. Army Engineer Waterways Experiment Station, Misc. Paper S-73-1, 221 p.

✓ Hamilton, W., 1978, Mesozoic tectonics of the western United States, in Howell, D.G., and McDougall, K.A., eds., Mesozoic paleogeography of the western United States: Pacific section, Soc. Econ. Paleontol. and Mineral. Pacific Coast Paleogeography Smyposium 2, p. 33-70.

✓ Hooke, R., 1967, Processes on arid-region alluvial fans: Jour. Geol., v. 75, p. 438-460.

Hooke, R., 1968, Stead-state relationships on arid-region alluvial fans in closed basins: Amer. Jour. Sci., v. 266, p. 609-629.

✓ Johnson, M.G., 1977, Geology and mineral deposits of Pershing County, Nevada: Nevada Bur. Mines and Geol., Bull. 89, 115 p.

and Churchill

Keplinger and Associates, Inc., 1978, Interim evaluation of exploration and development status, geothermal potential and associated economics of Dixie Valley, Nevada: Rept. prepared for Millican Oil Company, Sept. 1978, 60 p.

Koizumi, C.J., Ryall, A., and Priestley, K.F., 1973, Evidence for a high-velocity lithospheric plate under northern Nevada: Seismol. Soc. of Amer. Bull., v. 63, no. 6, p. 2135-2144.

Lachenbruch, A.H., and Sass, J.H., 1978, Models of an extending lithosphere and heat flow in the Basin and Range province; in Smith, R.B., and Eaton, G.P., eds., Cenozoic tectonics and regional geophysics of the western Cordillera: The Geol. Soc. of Amer. Mem. 152, p. 209-250.

Larson, E.R., 1957, Minor features of the Fairview fault, Nevada: Bull. Seism. Soc. America, v. 47, no. 4, p. 377-385.

Meister, L.J., 1967, Seismic refraction study of Dixie Valley, Nevada; in U.S. Air Force Cambridge Research Labs. Spec. Rept. 66-848, 72 p.

Nevada Bureau of Mines and Geology, 1977, Aeromagnetic map of Nevada: Reno sheet: Nevada Bur. Mines and Geol., Map 54.

Packham, G.H., and Falvey, D.A., 1971, An hypothesis for the formation of marginal seas in the western Pacific; Tectonophysics 11, p. 79-109.

Page, B.M., 1965, Preliminary geologic map of a part of the Stillwater Range, Churchill County, Nevada: Nevada Bur. Mines, Map 28.

Riehle, J.R., McKee, E.H., and Speed, R.C., 1972, Tertiary volcanic centers, west-central Nevada: Geol. Soc. Amer. Bull., v. 83, p. 1383-1396.

Ritter, D.F., 1979, Alluvial fans and stream morphology; in Geomorphic application in Engineering Geology, short course at California State University-Los Angeles, November 1979, Chapter 3, p. 21-45.

Ryall, A., and Malone, S.D., 1971, Earthquake distribution and mechanism of faulting in the Rainbow Mountain-Dixie Valley-Fairview Peak area, central Nevada: Jour. Geophys. Res., v. 76, p. 7241-7248.

Ryall, A., Slemmons, D.B., and Gedney, L., 1966, Seismicity, tectonism, and surface faulting in the western United States during historic time. Seismol. Soc. of Amer. Bull., v. 56, no. 5, p. 1105-1135.

Sanders, C.O., and Slemmons, D.B., 1979, Recent crustal movements in the central Sierra Nevada-Walker Lane region of California-Nevada: Part III , the Olinghouse fault zone: Tectonophysics, v. 52, p. 585-597.

Senturion Sciences, 1977, High-precision multi-level aeromagnetic survey over Dixie Valley, Nevada: Rept. prepared for Southland Royalty Company, Part I, Oct. 1977.

Senturion Sciences, 1978, High-precision multi-level aeromagnetic survey over Dixie Valley, Nevada: Rept. prepared for Southland Royalty Company, Part II, June, 1978.

Slemmons, D.B., 1957a, Map of Dixie Valley-Fairview Peak earthquakes of December 16, 1954: Publ. by Pacific Fire Rating Bureau.

Slemmons, D.B., 1957b, Geological effects of the Dixie Valley-Fairview Peak, Nevada earthquakes of December 15, 1954: Seis. Soc. America Bull., v. 47, no. 4, p. 353-375.

Slemmons, D.B., 1966, Guidebook for Nevada earthquake areas: Prepared for 2nd U.S.-Japan Conf. on Research related to Earthquake prediction, and the National Science Found. Conf. on Earthquakes and Earthquake Engineering, June, 1966, 79 p.

Slemmons, D.B., 1969, New Methods for studying regional seismicity and surface faulting: Geoscience, v. 10, Art. 1, p. 91-103.

Slemmons, D.B., in press, Design earthquake magnitudes for the western Great Basin: U.S.G.S. Open-file report.

Slemmons, D.B., Jones, A.E. and Gimlett, J.I., 1965, Catalog of Nevada earthquakes, 1852-1960, Bull. Seismo. Soc. of Amer. Bull., v. 55, no. 2, p. 537-583.

Slemmons, D.B., Van Wormer, D., Bell, E.J., and Silberman, M.L., 1979, Recent crustal movements in the Sierra Nevada-Walker Lane region of California-Nevada: Part I, rate and style of deformation: Tectonophysics 52, p. 561-570.

Smith, R.B., 1978, Seismicity, crustal structure, and intraplate tectonics of the interior of the western Cordillera: in Smith, R.B., and Eaton, G.P., eds., Cenozoic tectonics and regional geophysics of the western Cordillera: The Geol. Soc. of Amer. Mem. 152, p. 111-144.

Smith, R.B., and Lindh, A.G., 1978, Fault-plane solutions of the western United States: A compilation: in Smith, R.B., and Eaton, G.P., eds., Cenozoic tectonics and regional geophysics of the western Cordillera: The Geol. Soc. of Amer. Mem. 152, p. 107-109.

Smith, R.B., and Sbar, M.L., 1974, Contemporary tectonics and seismicity of the western United States with emphasis on the Intermountain seismic belt: Geol. Soc. of Amer. Bull., v. 85, p. 1205-1218.

Smith, T.E., 1967, Aeromagnetic measurements in Dixie Valley, Nevada: Implications regarding Basin-Range structure, in U.S. Air Force Cambridge Research Labs. Spec. Rpt. 66-848, 23 p.

Smith, T.E., 1968, Aeromagnetic measurements in Dixie Valley, Nevada: Implications on Basin-Range structure: Jour. Geophysical Res., v. 73, no. 4, p. 1321-1331.

Speed, R.C., 1976, Geologic map of the Humboldt Lopolith and surrounding terrain, Nevada: U.S. Geol. Survey Map MC-14, 4 p.

Speed, R.C., and Armstrong, R.L., 1971, Potassium-argon ages of some minerals from igneous rocks of western Nevada: Isochron/West, no. 1, p. 1-8.

Stewart, J.H., 1971, Basin and Range structure: a system of horsts and grabens produced by deep-seated extension: Geol. Soc. Amer. Bull., 82, p. 1019-1044.

Stewart, J.H., 1978, Basin-Range structure in western North America--a review, in Smith, R.B., and Eaton, G.P., eds., Cenozoic tectonics and regional geophysics of the western Cordillera: Geol. Soc. Amer. Mem. 152, p. 1-32.

Tchalenko, J.S., 1970, Similarities between shear zones of different magnitudes: Geol. Soc. Amer. Bull., v. 81, p. 1625-1640.

Thompson, G.A., and Burke, D.B., 1973, Rate and direction of spreading in Dixie Valley, Basin and Range Province, Nevada: Geol. Soc. Amer. Bull., v. 84, p. 627-632.

Thompson, G.A., and Burke, D.B., 1974, Regional geophysics of the Basin and Range Province: Ann. Rev. Earth and Planetary Sci., v. 2, p. 213-238.

Thompson, G.A., Meister, L.J., Herring, A.T., Smith, T.E., Burke, D.B., Kovach, R.L., Burford, R.O., Salehi, A., and Wood, M.D., 1967, Geophysical study of the Basin-Range structure, Dixie Valley region, Nevada: U.S. Air Force Cambridge Research Labs. Spec. Rept. 66-848.

Trexler, D.T., Bell, E.J., and Roquemore, G.R., 1978, Evaluation of lineament analysis as an exploration technique for geothermal energy, western and central Nevada: Rept. for U.S. Dept. of Energy, NVO-0671-2, 78 p.

Wallace, R.E., 1977, Profiles and ages of young fault scarps, north-central Nevada: Geol. Soc. Amer. Bull., v. 88, p. 1267-1281.

Wallace, R.E., 1978a, Geometry and rates of change of fault-generated range fronts, north-central Nevada: U.S.G.S. Geol. Survey, v. 6, no. 5, p. 637-650.

Wallace, R.E., 1978b, Patterns of faulting and seismic gaps in the Great Basin province, U.S.G.S. Open-file Report 78-943, 12 p.

Wallace, R.E., 1980a, Tectonic analysis of active faults: Report 9900-01270 in U.S.G.S., Menlo Park Semi-annual Technical Report, October 1, 1979-March 31, 1980, section H-5, 3 p.

Wallace, R.E., 1980b, Map of fault scarps formed during earthquake of October 2, 1915, Pleasant Valley, Nevada, and other young fault scarps, U.S.G.S. Open-file Report 80-608.

Willden, R., and Speed, R.C., 1974, Geology and mineral deposits of Churchill County, Nevada: Nevada Bur. Mines and Geol. Bull. 83.

Wright, L., 1976, Late Cenozoic fault patterns and stress fields in the Great Basin and westward displacement of the Sierra Nevada block: Geology, v. 4, p. 489-494.

A P P E N D I X   A

Grain-Size Distribution Diagrams for Selected Geomorphic Surface Samples

(Locations for sample sites are indicated on Plate III).

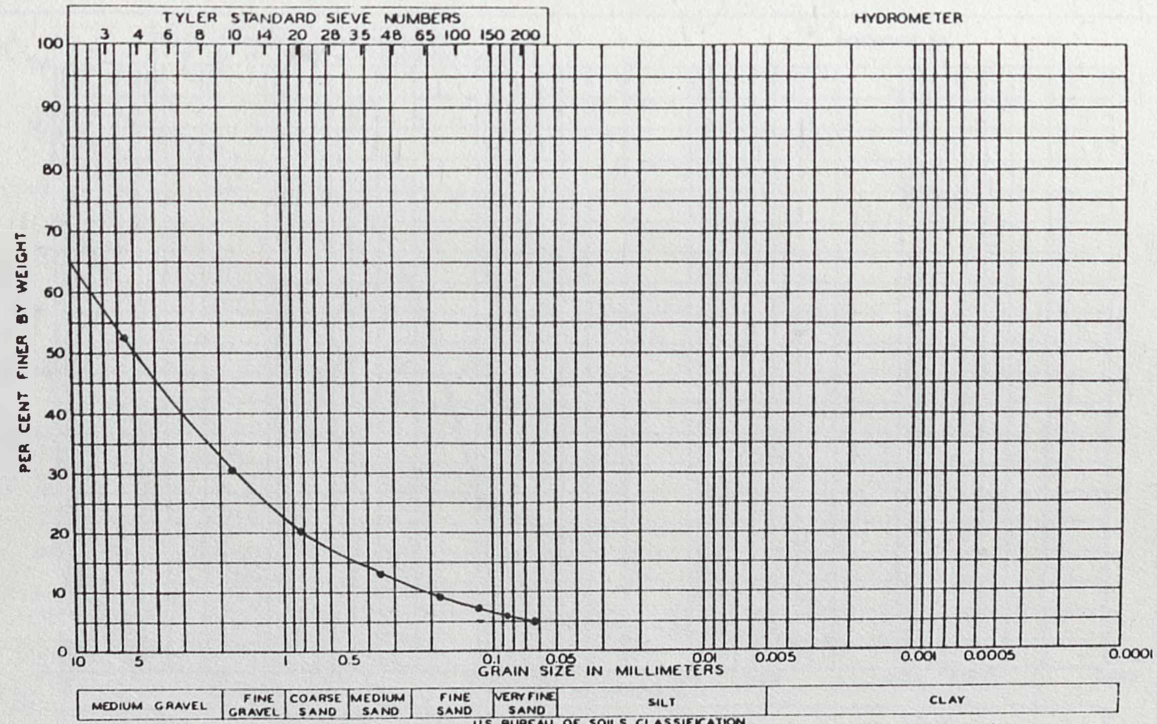

PROJECT ________ BORING NO ________ SAMPLE NO 1

DEPTH ______ ELEVATION ______ REMARKS head-active fan-west side

GRAIN SIZE DISTRIBUTION DIAGRAM

DCL-8

SOILTEST INCORPORATED • 2205 LEE STREET • EVANSTON, ILLINOIS, U.S.A.

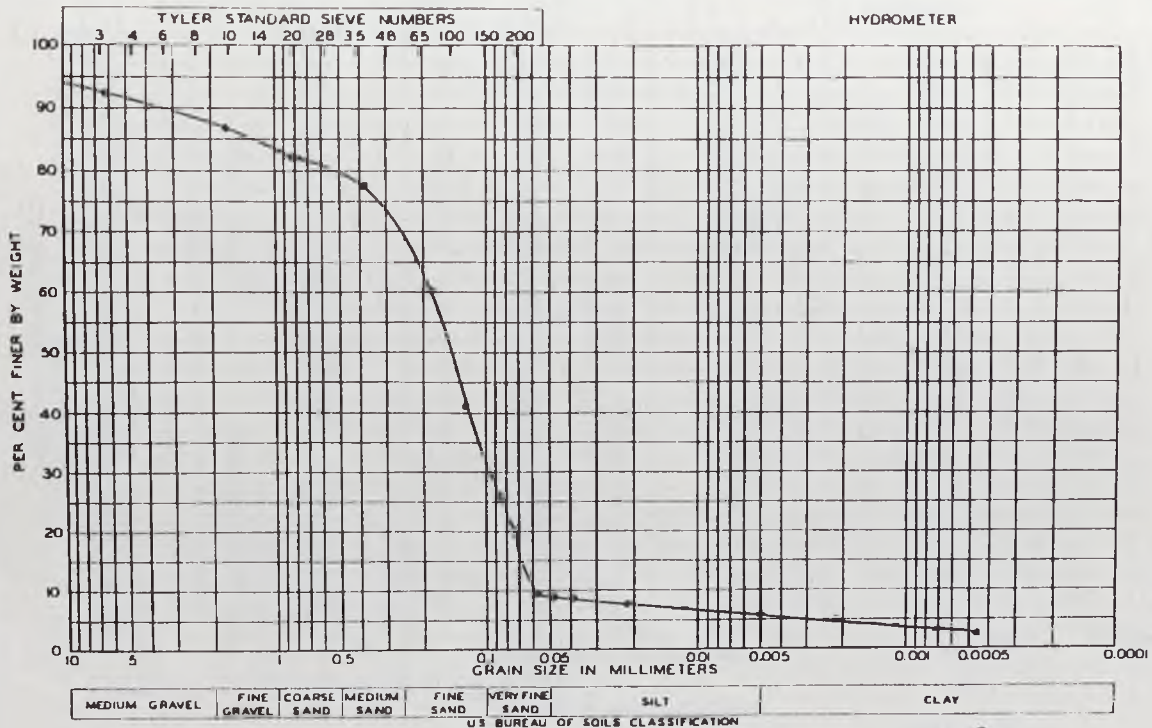

PROJECT ______ BORING NO ______ SAMPLE NO 2

DEPTH ______ ELEVATION ______ REMARKS toe-active fan-east side

GRAIN SIZE DISTRIBUTION DIAGRAM

DCL - 8

SOILTEST INCORPORATED • 2205 LEE STREET • EVANSTON, ILLINOIS, U.S.A.

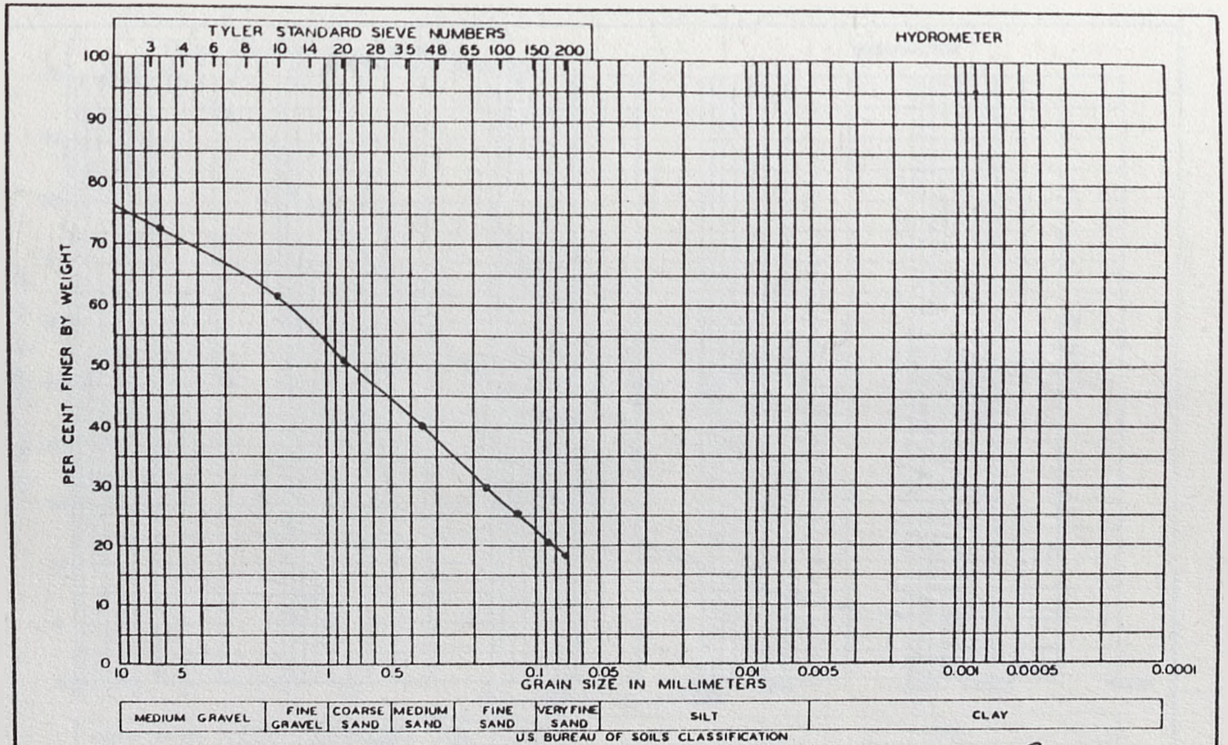

PROJECT ________ BORING NO ________ SAMPLE NO 3

DEPTH ______ ELEVATION ______ REMARKS middle-active fan-west side

GRAIN SIZE DISTRIBUTION DIAGRAM

DCL - 8

SOILTEST INCORPORATED • 2205 LEE STREET • EVANSTON, ILLINOIS, U.S.A.

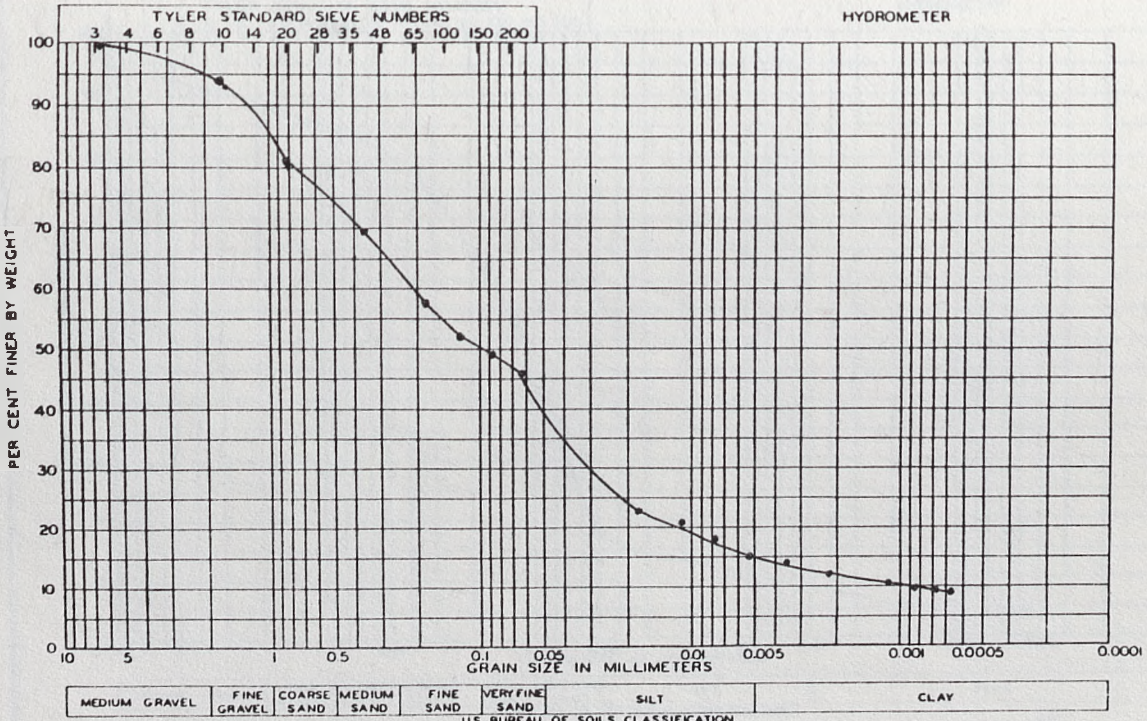

PROJECT ______ BORING NO ______ SAMPLE NO 4

DEPTH ______ ELEVATION ______ REMARKS valley fill-north end

GRAIN SIZE DISTRIBUTION DIAGRAM

DCL-8

SOILTEST INCORPORATED • 2205 LEE STREET • EVANSTON, ILLINOIS, U.S.A.

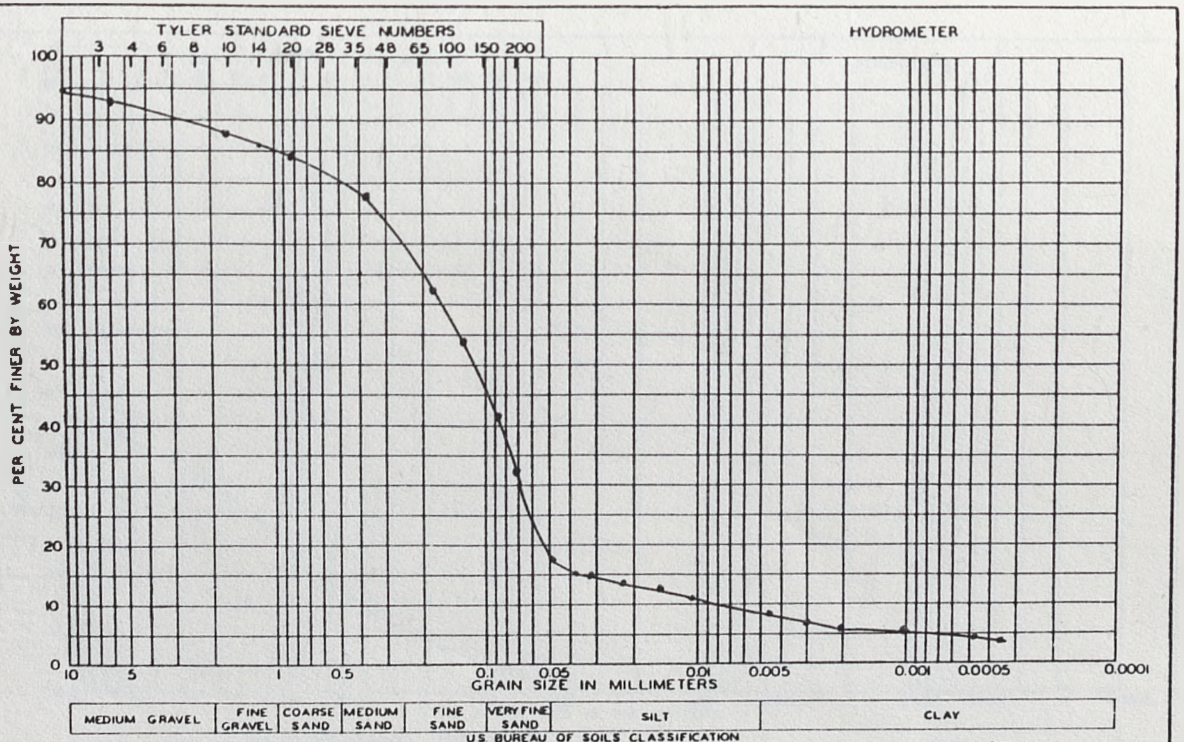

PROJECT ______ BORING NO ______ SAMPLE NO 5

DEPTH ______ ELEVATION ______ REMARKS middle-active fan-Shoshone Creek

GRAIN SIZE DISTRIBUTION DIAGRAM

DCL - 8

SOILTEST INCORPORATED • 2205 LEE STREET • EVANSTON, ILLINOIS, U.S.A.

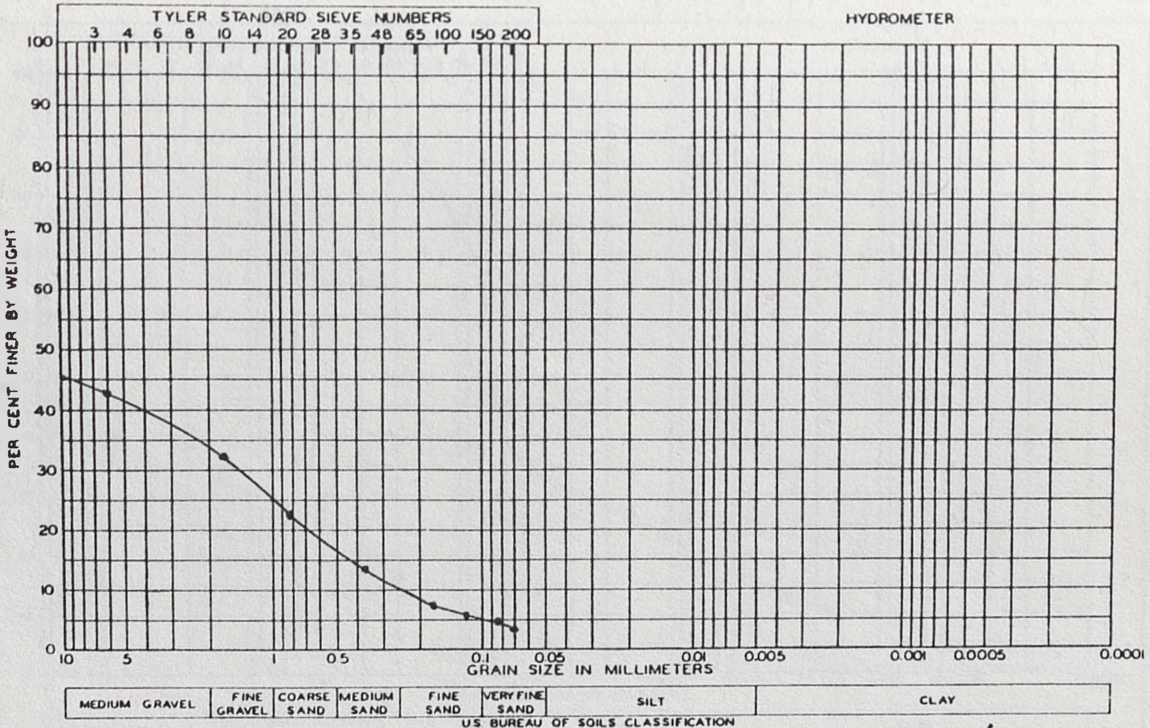

PROJECT ____ BORING NO ____ SAMPLE NO 6

DEPTH ____ ELEVATION ____ REMARKS delta-Mississippi Canyon

GRAIN SIZE DISTRIBUTION DIAGRAM

DCL-8

SOILTEST INCORPORATED • 2205 LEE STREET • EVANSTON, ILLINOIS, U.S.A.

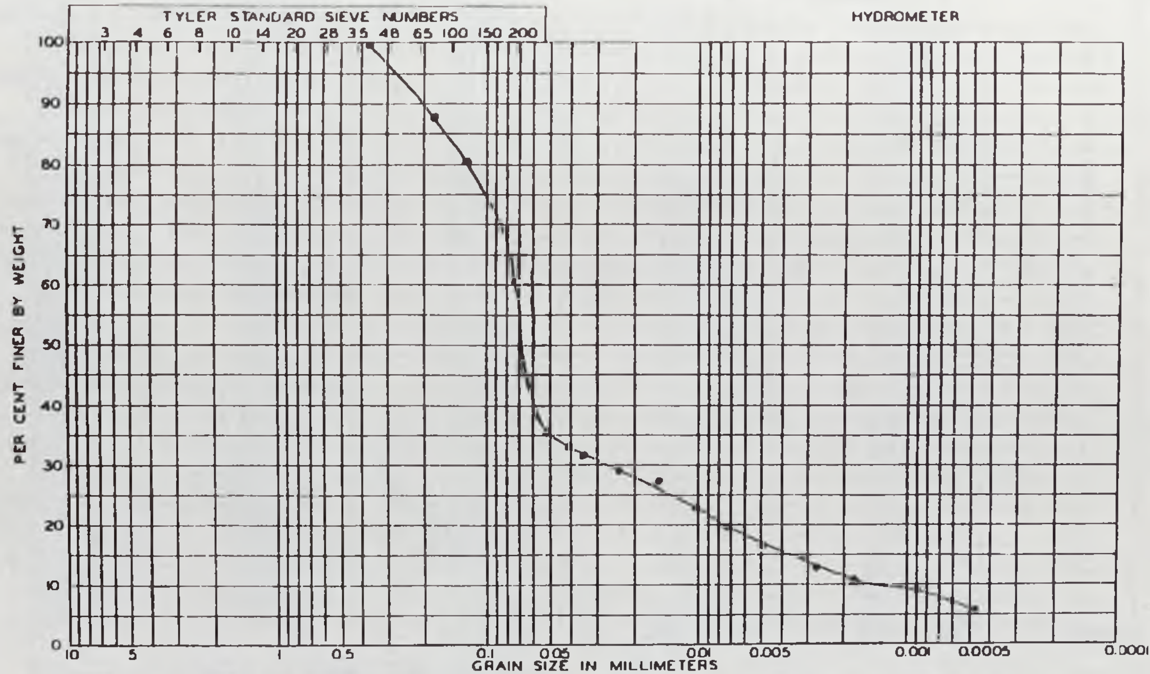

MEDIUM GRAVEL	FINE GRAVEL	COARSE SAND	MEDIUM SAND	FINE SAND	VERY FINE SAND	SILT	CLAY

US BUREAU OF SOILS CLASSIFICATION

PROJECT________ BORING NO ______ SAMPLE NO 7

DEPTH_____ ELEVATION_____ REMARKS valley fill-west side

GRAIN SIZE DISTRIBUTION DIAGRAM

DCL - 8

SOILTEST INCORPORATED • 2205 LEE STREET • EVANSTON, ILLINOIS, U.S.A.

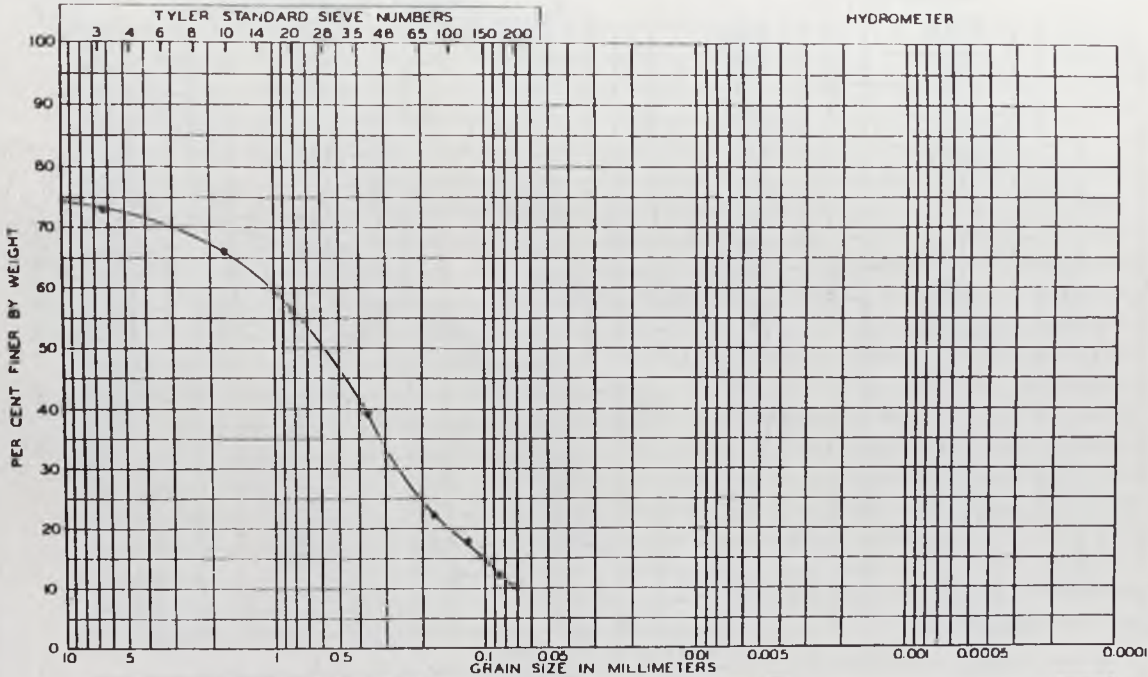

MEDIUM GRAVEL	FINE GRAVEL	COARSE SAND	MEDIUM SAND	FINE SAND	VERY FINE SAND	SILT	CLAY

US BUREAU OF SOILS CLASSIFICATION

PROJECT ______ BORING NO ______ SAMPLE NO 8

DEPTH ______ ELEVATION ______ REMARKS toe-active fan-west side

GRAIN SIZE DISTRIBUTION DIAGRAM

DCL - 8

SOILTEST INCORPORATED • 2205 LEE STREET • EVANSTON, ILLINOIS, U.S.A.

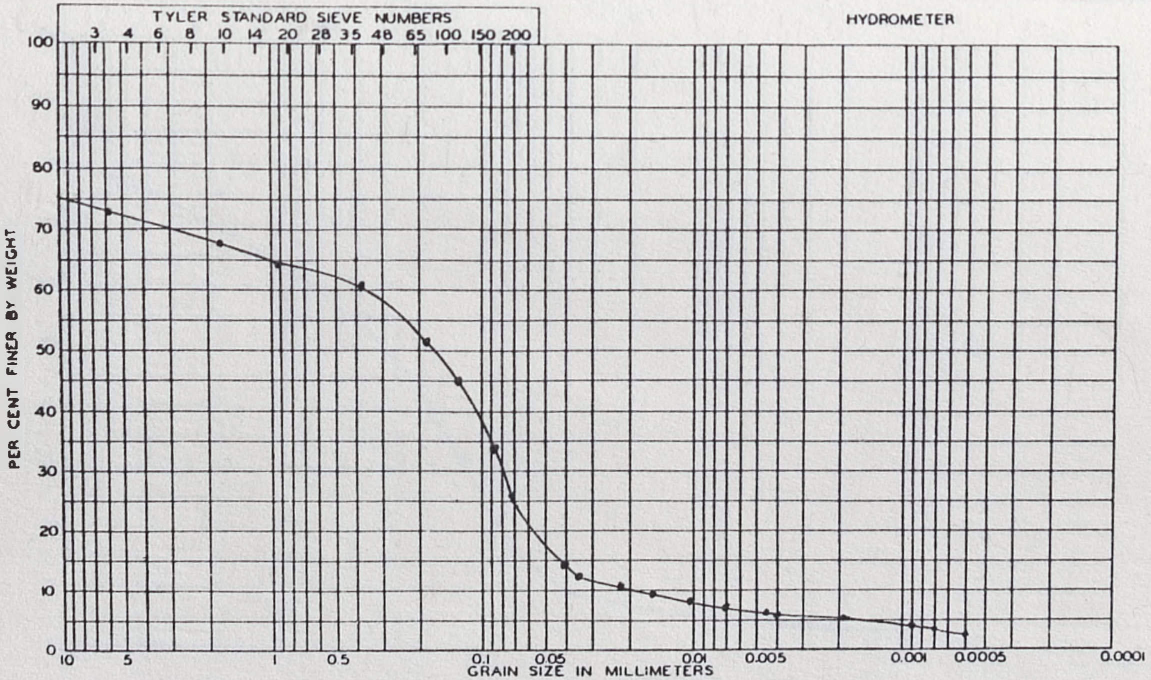

MEDIUM GRAVEL	FINE GRAVEL	COARSE SAND	MEDIUM SAND	FINE SAND	VERY FINE SAND	SILT	CLAY

US BUREAU OF SOILS CLASSIFICATION

PROJECT ______ BORING NO ______ SAMPLE NO 9

DEPTH ______ ELEVATION ______ REMARKS toe-inactive fan-west side

GRAIN SIZE DISTRIBUTION DIAGRAM

DCL - 8

SOILTEST INCORPORATED • 2205 LEE STREET • EVANSTON, ILLINOIS, U.S.A.

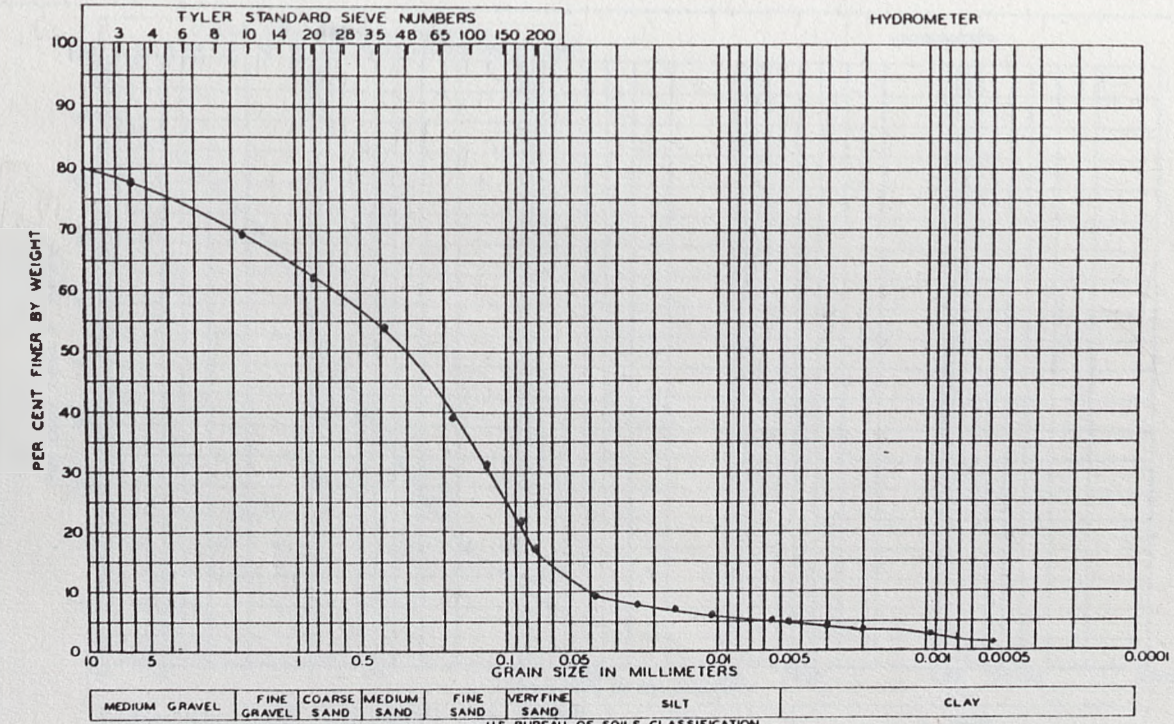

PROJECT ________ BORING NO ________ SAMPLE NO 10

DEPTH ______ ELEVATION ______ REMARKS head-inactive fan-west side

GRAIN SIZE DISTRIBUTION DIAGRAM

DCL - 8

SOIL TEST INCORPORATED • 2205 LEE STREET • EVANSTON, ILLINOIS, U.S.A.

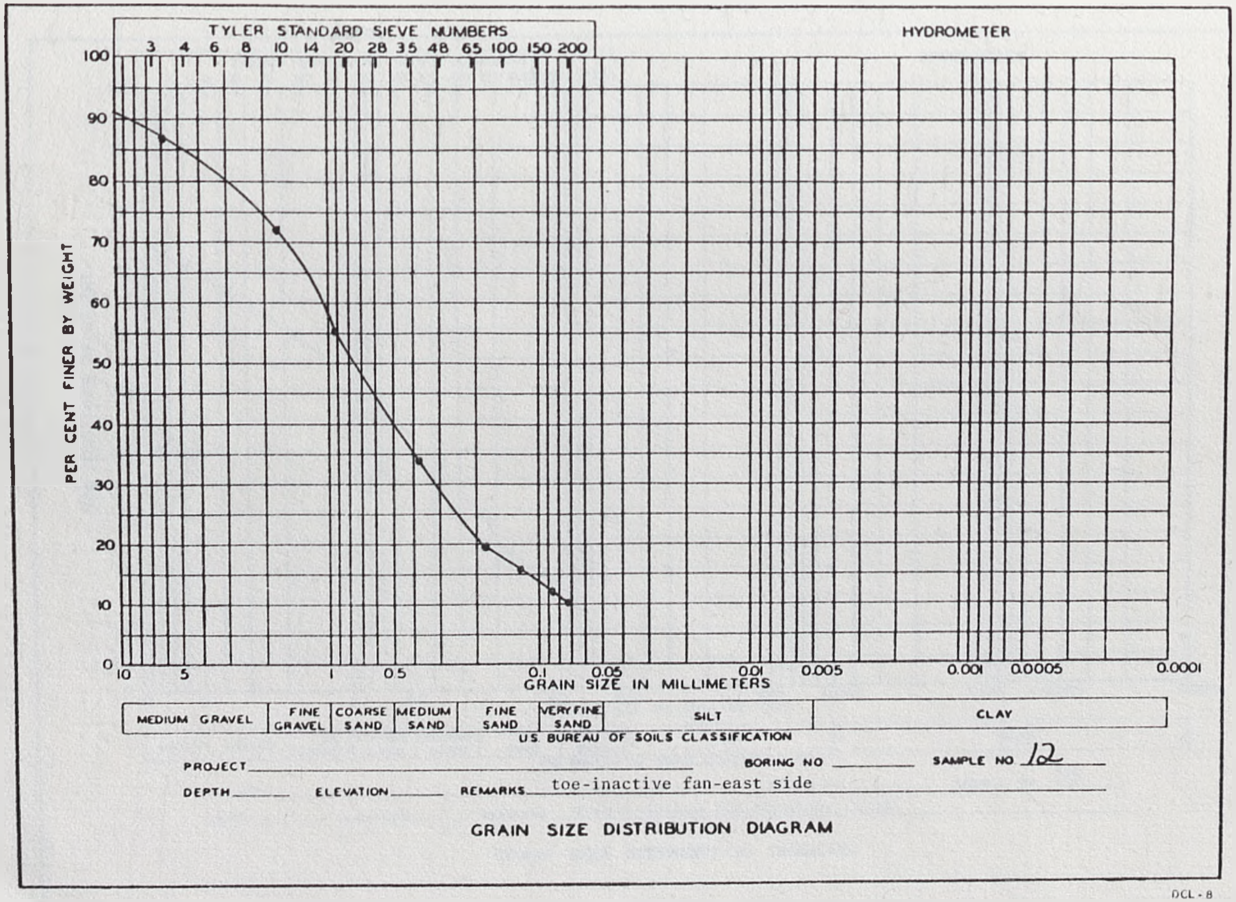

DCL-8

SOILTEST INCORPORATED • 2205 LEE STREET • EVANSTON, ILLINOIS, U.S.A.

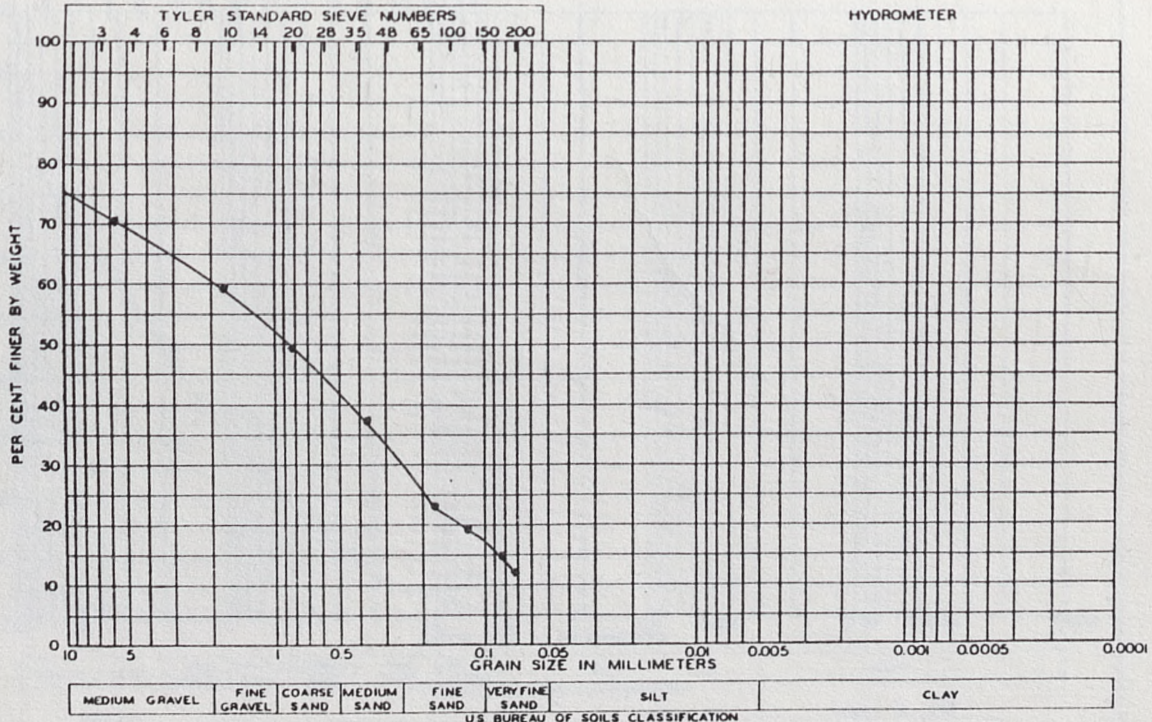

PROJECT_____ BORING NO _____ SAMPLE NO 13

DEPTH_____ ELEVATION_____ REMARKS middle-active fan-Shoshone Creek

GRAIN SIZE DISTRIBUTION DIAGRAM

DCL-8

SOILTEST INCORPORATED • 2205 LEE STREET • EVANSTON, ILLINOIS, U.S.A.

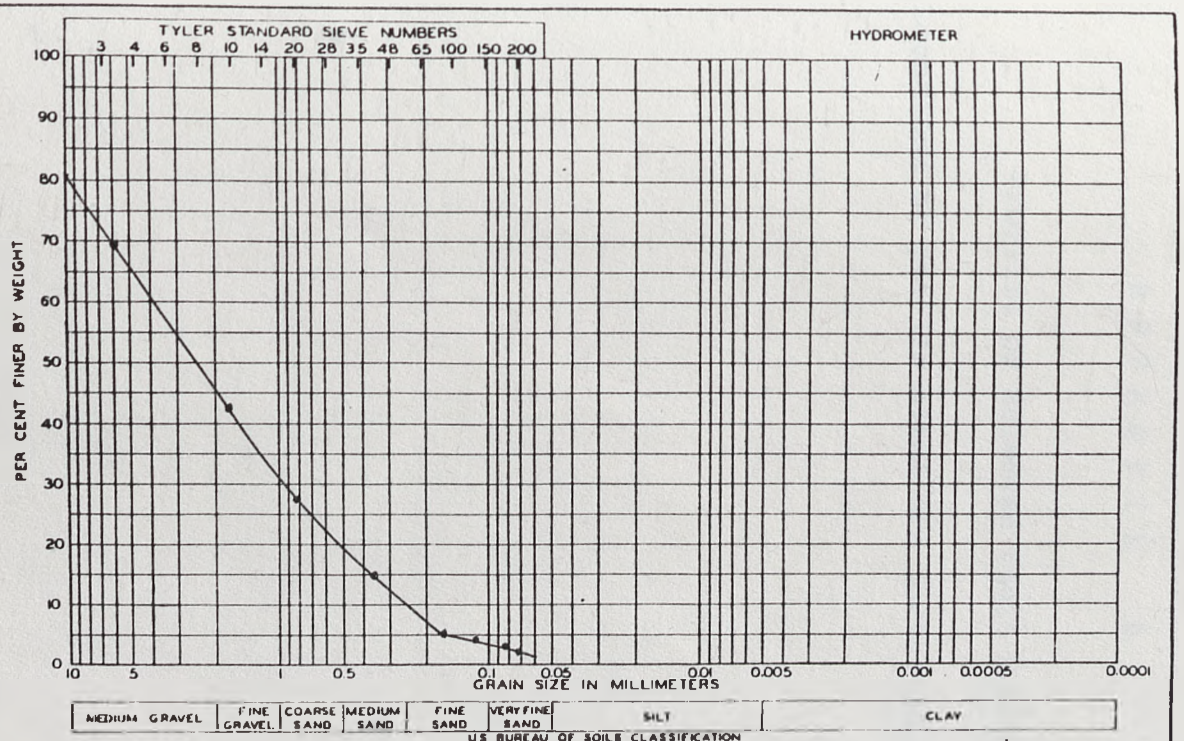

PROJECT ______ BORING NO ______ SAMPLE NO 14

DEPTH ______ ELEVATION ______ REMARKS delta-east side

GRAIN SIZE DISTRIBUTION DIAGRAM

DCL - 8

SOILTEST INCORPORATED • 2205 LEE STREET • EVANSTON, ILLINOIS, U.S.A.

A P P E N D I X   B

Profiles of Selected Fault Scarps

(Locations of profile sites are indicated on Plate IV).

Fault Scarp Profile # 1

o = inflection point

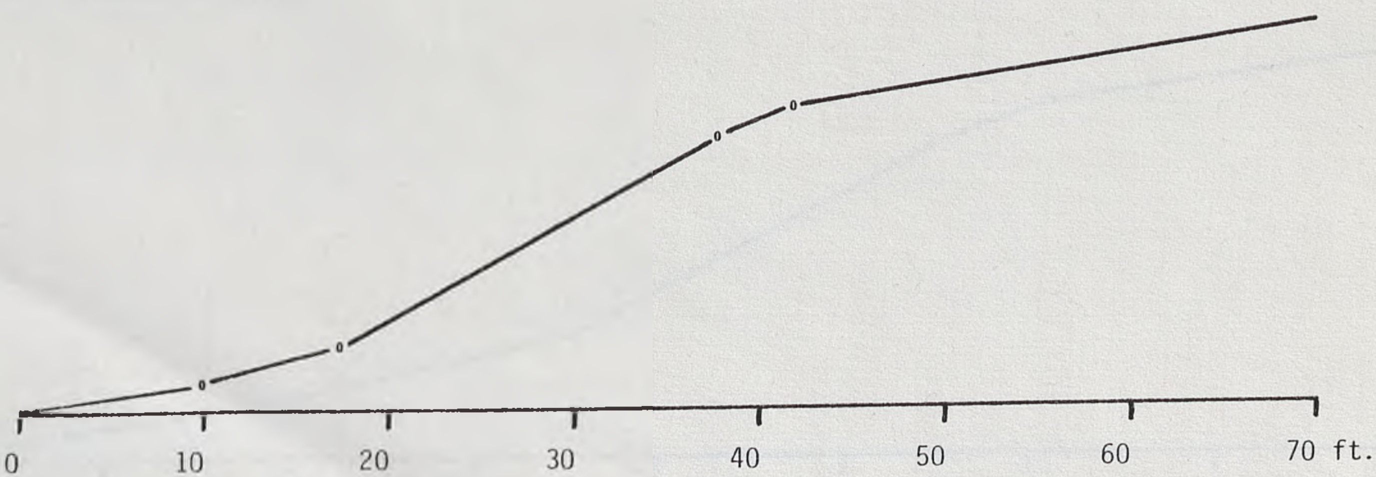

Fault Scarp Profile # 2

o = inflection point

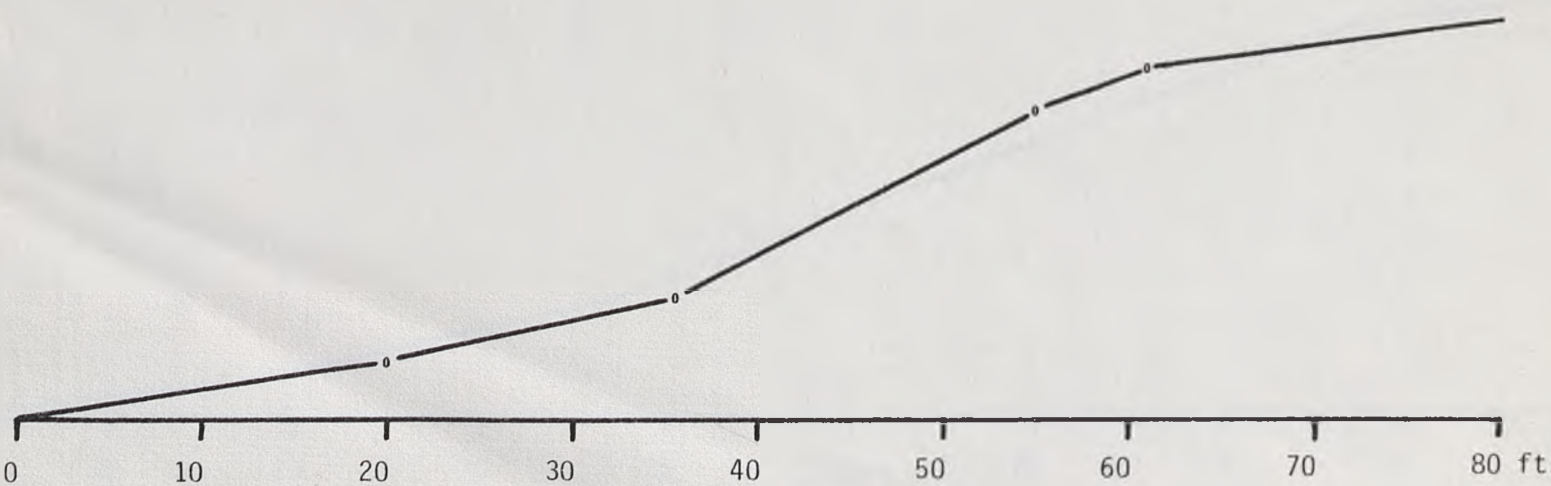

Fault Scarp Profile # 3

o = inflection point

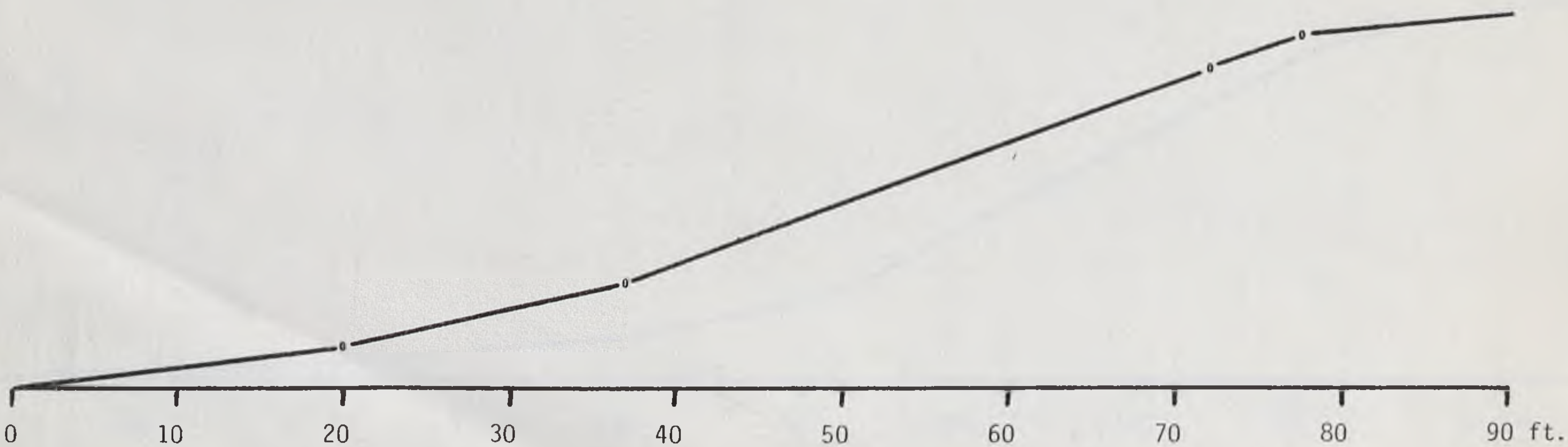

Fault Scarp Profile # 4

o = inflection point

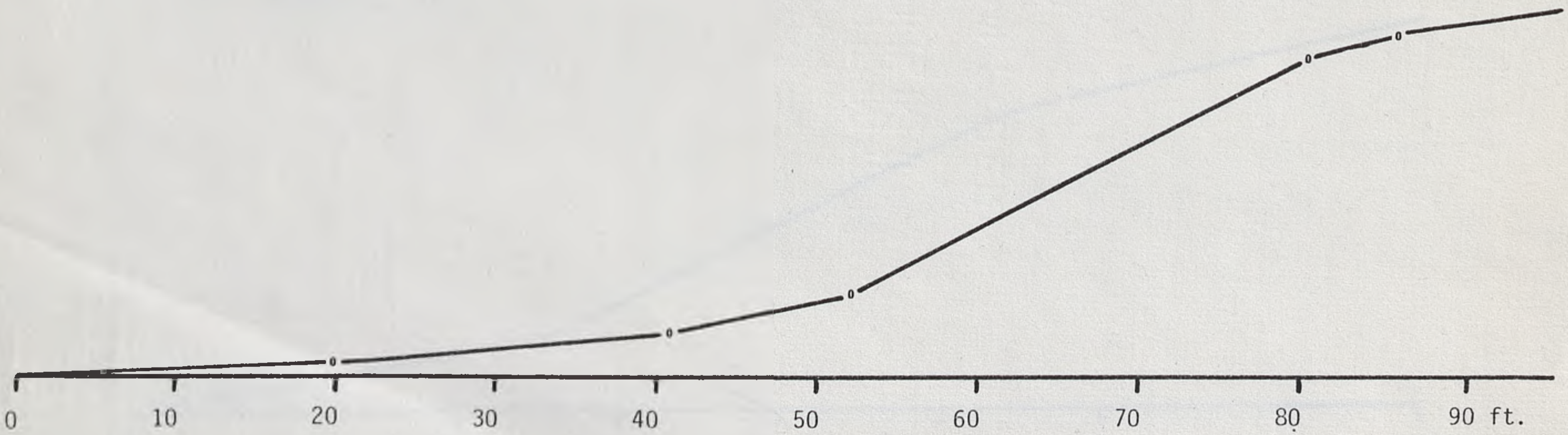

Fault Scarp Profile # 5

o = inflection point

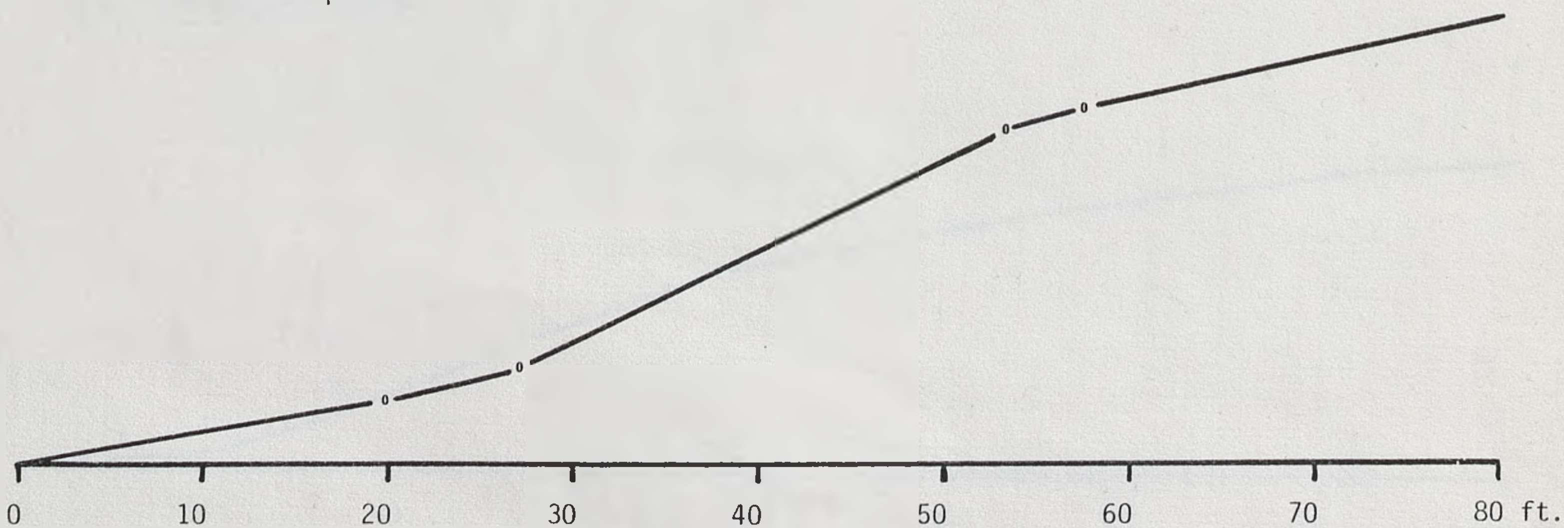

Fault Scarp Profile # 6

o = inflection point